agriculture

MDPI

Article

Functional Interpretation of Cross-Talking Pathways with Emphasis on Amino Acid Metabolism in Rhizosphere Microbiome of the Wild Plant *Moringa oleifera*

Manal A. Tashkandi [1], Rewaa S. Jalal [2], Lina Baz [3], Mohammed Y. Refai [1], Ashwag Shami [4], Ruba Abdulrahman Ashy [2], Haneen W. Abuauf [5], Fatimah M. Alshehrei [6], Fawzia A. Alshubaily [3], Aminah A. Barqawi [7], Sahar Alshareef [8] and Aala A. Abulfaraj [9,*]

1 Department of Biochemistry, College of Science, University of Jeddah, Jeddah 21493, Saudi Arabia
2 Department of Biology, College of Science, University of Jeddah, Jeddah 21493, Saudi Arabia
3 Department of Biochemistry, Faculty of Science, King AbdulAziz University, Jeddah 21589, Saudi Arabia
4 Department of Biology, College of Science, Princess Nourah bint Abdulrahman University, P.O. Box 84428, Riyadh 11617, Saudi Arabia
5 Department of Biology, Faculty of Applied Science, Umm Al-Qura University, Makkah 24381, Saudi Arabia
6 Department of Biology, Jumum College University, Umm Al-Qura University, P.O. Box 7388, Makkah 21955, Saudi Arabia
7 Department of Chemistry, Al-Leith University College, Umm Al Qura University, Makkah 28434, Saudi Arabia
8 Department of Biology, College of Science and Arts at Khulis, University of Jeddah, Jeddah 21921, Saudi Arabia
9 Biological Sciences Department, College of Science & Arts, King Abdulaziz University, Rabigh 21911, Saudi Arabia
* Correspondence: aaabulfaraj@kau.edu.sa

check for updates

Citation: Tashkandi, M.A.; Jalal, R.S.; Baz, L.; Refai, M.Y.; Shami, A.; Ashy, R.A.; Abuauf, H.W.; Alshehrei, F.M.; Alshubaily, F.A.; Barqawi, A.A.; et al. Functional Interpretation of Cross-Talking Pathways with Emphasis on Amino Acid Metabolism in Rhizosphere Microbiome of the Wild Plant *Moringa oleifera*. *Agriculture* **2022**, *12*, 1814. https://doi.org/10.3390/agriculture12111814

Academic Editors: Tibor Szili-Kovács and Tünde Takács

Received: 2 October 2022
Accepted: 25 October 2022
Published: 31 October 2022

Abstract: The functional processes and mutual benefits of the wild plant *Moringa oleifera* and its rhizosphere microbiome were studied via metagenomic whole-genome shotgun sequencing (mWGS) in comparison with a bulk soil microbiome. The results indicated high gene abundance of the four KEGG categories, "Cellular Processes", "Environmental Information Processing", "Genetic Information Processing", and "Metabolism", in the rhizosphere microbiome. Most of the enriched enzymes in rhizobacteria are assigned to the pathway "Amino acids metabolism", where soil-dwelling microbes use amino acids as a defense mechanism against phytopathogens, while promoting growth, colonizing the cohabiting commensal microbes and conferring tolerance against abiotic stresses. In the present study, it was proven that these beneficial microbes include *Bacillus subtilis*, *Pseudomonas fluorescens*, and *Escherichia coli*. Mineral solubilization in these rhizobacteria can make nutrients available for plant utilization. These rhizobacteria extensively synthesize and metabolize amino acids at a high rate, which makes nitrogen available in different forms for plants and microbes. Amino acids in the rhizosphere might stand mainly as an intermediate switcher for the direction of the soil nitrogen cycle. Indole acetic acid (IAA) was proven to be synthesized by these beneficial rhizobacteria via route indole-3-pyruvate (IPyA) of the pathway "Tryptophan metabolism". This hormone might stand as a shuttle signaling molecule between *M. oleifera* and its rhizobacteria. Tryptophan is also metabolized to promote other processes with important industrial applications. Rhizobacteria were also proven to breakdown starch and sucrose into glucose, which is the primary metabolic fuel of living organisms. In conclusion, we assume that the metabolic processes in the rhizosphere microbiome of this wild plant can be eventually utilized in boosting the sustainability of agriculture applications and the plant's ability to benefit from soil nutrients when they are not in the form available for plant root absorption.

Keywords: mWGS; phytopathogen; rhizobacteria; solubilization; tryptophan; glucose

1. Introduction

Moringa oleifera is a small tree of the family Moringaceae [1] that is grown in the wild in Saudi Arabia [2,3]. It is an edible plant with a high nutritional value, as it is rich in proteins, vitamins, oils, fatty acids, micro/macro elements, and phenolics [4]. This plant also has important medicinal properties and is considered to be a promising healer due to its richness in anti-inflammatory, anti-microbial, anti-oxidant, anti-cancer, and anti-ulcer compounds [2,4]. Extensive research on this wild plant might lead to the recovery of novel agents to be used commercially to lower human blood sugar and cholesterol levels, and in the treatment of human cancer and cardiovascular diseases, in addition to many other medical applications [4]. This wild plant not only provides beneficial characteristics in medicine and pharmaceuticals, but can also provide a model as to how plants benefit from their rhizobiomes and maintain good performance, especially under adverse conditions.

In order to obtain accurate figures on the rhizobiome signatures of wild plant species, high-throughput technology ought to be utilized. Next-generation sequencing at the level of 16S rRNA amplicon sequencing and metagenomic whole-genome shotgun sequencing (mWGS) can allow us to investigate in depth the structure and function of the microbial community in a plant's rhizosphere. The advantages of the 16S rRNA approach include the existence of informative databases (e.g., Greengenes [5] and SILVA [6]), which harbor marker genes from millions of taxa. However, the problem with the 16S rRNA approach is that it does not capture viruses as they do not have conserved gene analogs to 16S or 18S rRNA genes that can be used as marker genes at different taxonomic ranks. Chen and colleagues [7] and other researchers [8,9] indicated that the marker gene sequencing approach is subject to bias and low sensitivity, and lacks real functional information from the studied microbiome. Nevertheless, results based on mWGS are more precise and can result in the generation of high-quality draft bacterial genomes, on one hand, and in the actual gene abundance and metabolic processes of microbiomes in a given ecosystem, on the other [10–16].

Rhizosphere soil is the site by which plant and microbes interact and is regarded as one of the most active interfaces on Earth [17–19]. As in that of a human, a plant's rhizosphere microbiome is considered to be a second genome that promotes health and growth under normal and adverse conditions [19]. Many studies have demonstrated that rhizosphere microbiomes can be influenced by plant root architecture and the type of released exudates, which play a major role in attracting bacteria to the rhizosphere region in addition to being substrates for bacterial functions [20,21]. Accordingly, it is expected that microbiome signatures will differ based on the type of soil (e.g., bulk or rhizosphere) and on the genetic makeup of the plant that hosts the microbiome in its rhizosphere region [22]. Agricultural practices that are applied during the growth of crop plants significantly affect the signature of the native plant soil rhizosphere microbiome, as practices might result in losing microbes with important features, like plant growth enhancement and disease protection [23–26]. The rhizosphere microbiomes of wild plants, like that of *M. oleifera*, are maintained in their native environment in terms of structure, pattern of microbial community assembly, molecular functions, plant-microbe interactions, and dynamics of microbial evolution [27–31].

The present study aims to use the mWGS approach to detect the metabolic processes and core metabolites of cross-talking pathways in the rhizosphere versus bulk soil microbiomes of the wild plant *M. oleifera* that indicate the types of plant-microbe interactions.

2. Materials and Methods

2.1. Sample Collection and DNA Extraction

Samples were collected in three replicates from the rhizosphere soil of single-grown *M. oleifera* plants and surrounding bulk soil growing naturally in the North Western region of the Mecca district of Saudi Arabia, near the red sea coast (21°12′17.8″ N 39°31′26.4″ E) [3]. The collection spots of the two soil types received no rainfall for >3 months prior to sample collection. For rhizosphere soil collection, lateral roots were cut at ~10–30 cm of

depth. Then, soil of ≤1 cm away from the root that did not physically adhere to the root was collected. Meanwhile, bulk soil samples were taken ≥10 m away from the growing *M. oleifera* plants to avoid the two soil types being mixed up. Then, soil samples were immediately put in liquid nitrogen, transported to the lab, and stored at −20 °C until genomic and transcriptomic extractions took place [32]. Then, the DNAs of rhizosphere and bulk soil microbiome samples were extracted using the CTAB/SDS method. The purity and integrity of the extracted DNAs were checked using 1% agarose gel electrophoresis. As a prerequisite for whole-metagenome shotgun sequencing (mWGS), the concentration of each DNA sample was adjusted to 10 ng/μL using a dsDNA Assay kit (Life Technologies, Carlsbad, CA, USA).

2.2. Whole-Genome Shotgun Sequencing and Bioinformatics Analysis

A total of 1 μg of extracted DNA from the samples was shipped to Novogene Co. (Singapore) for metagenomic whole-genome shotgun sequencing (mWGS). Then, library preparation was constructed, and the DNAs were sequenced on an Illumina HiSeq 2500 platform. Recovered raw data were deposited in the European Nucleotide Archive (ENA) (https://www.ebi.ac.uk/ena/browser/ (accessed on 30 September 2022)) and the received accession Nos. ERR10100770-72 for rhizosphere soil samples R1, R2 and R3, and ERR10100773-74 and ERR10100781 for bulk soil samples S1, S2 and S3, respectively. After physical fractionation of DNAs and data pre-processing, low-quality bases (Q value ≤ 38) exceeding a 40-bp threshold were trimmed and removed. Reads with a number of Ns of 10 ≥ bp were removed. Then, the library was prepared using an Ultra DNA Library Prep kit for Illumina (NEB, Ipswich, MA, USA) and clean data were sequenced on an Illumina HiSeq 2500 platform. Generated reads were de novo assembled to recover scaffolds using MEGAHIT (K-mer = 55) and chimeras were removed as previously described [33–35]. Then, low abundant unassembled reads of all samples were gathered and assembled de novo to generate NOVO_MIX scaffolds that were cut off at "N" to obtain fragments, called "scaftigs" [33,36]. The mapping of clean data was conducted using Soap 2.21, then effective scaftigs that were presumably found in ≥2 samples were utilized further. Gene prediction was carried out for the recovered ORFs and scaftigs using MetaGeneMark [36], and the resultant genes were dereplicated using Cluster Database at High Identity with Tolerance (CD-HIT) [37,38]. Then, gene redundancy was removed using a greedy pairwise comparison [39] and non-redundant gene catalogues (nrGC) were constructed. Then, annotation was completed using the binning reference-based classification method MEGAN [40,41].

The functions of the coding metagenomic sequences of different microbiome samples were then inferred based on their similarity to sequences in the 18 Kyoto Encyclopedia of Genes and Genomes (KEGG) databases, of which KEGG PATHWAY, KEGG orthology (KO), and KEGG ENZYME (EC) are the core ones [42–46]. The KO database was used for detecting molecular functions represented as functional orthologs, while the KEGG PATHWAY database was used for pathway mapping that was comprised of three levels (e.g., 1, 2 and 3), and KEGG ENZYME (EC or enzyme commission) was used for functional annotation [34,39,47]. The three databases resulted in the recovery of a profile to describe the functions across and between groups of the two microbiome soil types at Levels 1, 2, and 3, as well as at Level EC. Based on the resulting table of functional abundance, cluster analysis was conducted based on the Bray-Curtis distance, and a bar plot and a principle component analysis (PCA) were carried out. Then, the abundance distributions of 35 selected, highly abundant functions were displayed using heatmaps at the three different KEGG Levels.

Validation of the gene abundance datasets that resulted from mWGS was conducted at the metatranscriptomic level, as previously described [48] via Maxima^{TM} SYBR Green/ROX qPCR, for three randomly selected highly abundant genes in addition to one non-existing gene in the rhizosphere microbiome of *M. oleifera*. Information about these genes at the National Center for Biotechnology Information (NCBI), along with sequences of primers designed using Netprimer software (http://www.premierbiosoft.com/netprimer/index.

html (accessed on 31 August 2022)), are described in Table S1. Then, the partial-length 16S rRNA of *Bacillus subtilis* was used in the reactions as the housekeeping gene.

3. Results

3.1. Validation and Fidelity Testing of KEGG Datasets

Validation of mWGS datasets was conducted via real-time PCR using four randomly selected genes. In alignment with the results of the deep sequencing of microbiomes surrounding *M. oleifera*, real-time PCR indicated that genes encoding the three enzymes with ECs 4.2.1.20, 4.1.1.28, and 3.1.3.25 showed higher abundance in the rhizosphere microbiome of *M. oleifera* than those in bulk soil microbiome (Figure S1), while the gene encoding EC 1.13.12.3 was not detected in either type of microbiome. The fidelity of KEGG datasets was tested by detecting the closeness among samples of each soil type at KEGG Levels 1, 2, 3, and EC via principal component analysis (PCA) (Figure 1).

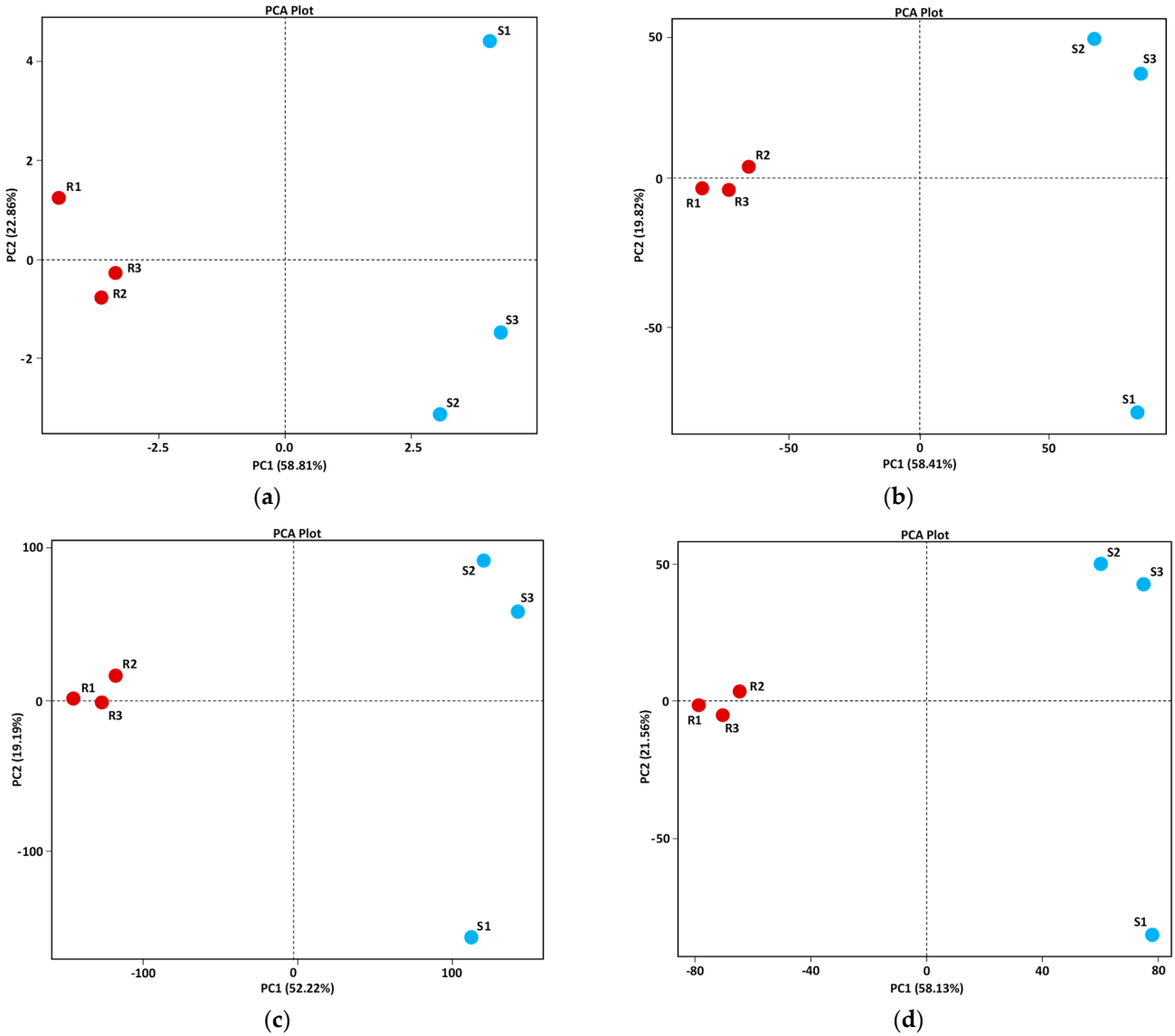

Figure 1. Principle component analysis (PCA) based on KEGG (Kyoto Encyclopedia of Genes and Genomes) database Levels 1 (**a**), 2 (**b**), 3 (**c**), and EC (**d**) referring to prokaryotic and eukaryotic microbes in microbiome samples of rhizosphere (R) and surrounding bulk (S) soils of *M. oleifera*.

Results showed discrete distances between microbiomes from the two soil types, where rhizosphere microbiome samples existed on the negative side of the PCA 1 (or PC1)

across the four levels, while bulk soil microbiome samples existed on the right side. For PC2, higher diversity was detected among samples from bulk soil microbiome compared with those of the rhizosphere soil. These data refer to the structure of microbiome and the gene abundance of the two soil types.

3.2. Description of Assembled Raw Sequence Data

The alignment results of assembled ORFs/scaftigs (or queries) versus analogue sequences (or subjects) in the NCBI referred to identity/mismatch, gap sizes (nt), and nucleotides assigning gene start and end points (Table S2). A total of 232,087 ORFs originating from one type of soil and 27,559 scaftigs (NOVO_MIX) present in one or the two types of soil were recovered. Queries have aligned with subjects whose lengths are between 27 and 2323 nt, have identities of 50–100%, and have mismatches of 0–941 nt. It is important to note that a given subject can have hits with more than one query. Examples include subject aaa:Acav_0403, which has hits with two queries, namely R3_754948 and R3_797052 (Table S2).

3.3. Differential Abundance of Genes Encoding KEGG Enzymes

The abundance of genes encoding enzymes in the KEGG category (Level 1) and sub-category (Level 2) levels across samples of either type of microbiome is shown in Figures 2a and 3a, respectively, while summarized in Figure S2. The results indicated high gene abundance of the four categories: "Cellular Processes", "Environmental Information Processing", "Genetic Information Processing" and "Metabolism". The numbers of highly abundant sub-categories in these categories are 2, 1, 1, and 4, respectively. Sub-categories of category "Cellular Processes" include "Cellular community-prokaryotes" and "Cell mobility", while that of "Environmental Information Processing" is sub-category "Membrane transport", that of "Genetic Information Processing" is sub-category "Translation", and those of "Metabolism" include sub-categories "Energy metabolism", "Carbohydrate metabolism", Biosynthesis of other secondary metabolites", and "Amino Acid metabolism" (Figures 2a, 3a and S2). Across these four categories and eight sub-categories, the gene abundance in the rhizosphere microbiome of *M. oleifera* was higher than that of samples from the bulk soil microbiome (Figure 2b, Figure 3b, Figures S3 and S4, respectively).

Gene abundance across and between soil microbiome types for 21 selected KEGG pathways from the eight sub-categories are shown in Figure 4a,b. Nine of these pathways referring to soil type microbiomes are displayed in Figure S5. The results indicated that the abundance of genes in the rhizosphere microbiome at the level of pathways for the eight sub-categories is higher than that of the bulk soil microbiome of *M. oleifera* (Figure 4b). Details of the selected 21 pathways from Figure 4 along with an additional pathway that is not enriched in the present study are shown in Table 1. Enriched enzymes in the 22 pathways are shown in Figures S6–S27. The additional pathway refers to a reaction, involving tryptophan and indole, that is not displayed in the pathway "Biosynthesis of various plant secondary metabolites" (Figure S20), although it is displayed in the pathway "Phenylalanine, tyrosine and tryptophan biosynthesis" (Figure S17). The boxes around the ECs of enzymes in these pathways are colored based on the level of enrichment, where red boxes indicate highly enriched enzymes in the rhizosphere microbiome, and blue boxes indicate highly enriched enzymes in the bulk soil microbiome of *M. oleifera*. Other colors refer to intermediate levels of gene abundance in both types of soil microbiomes. Detailed information regarding enzyme enrichment between soil microbiome types is shown in Table S11.

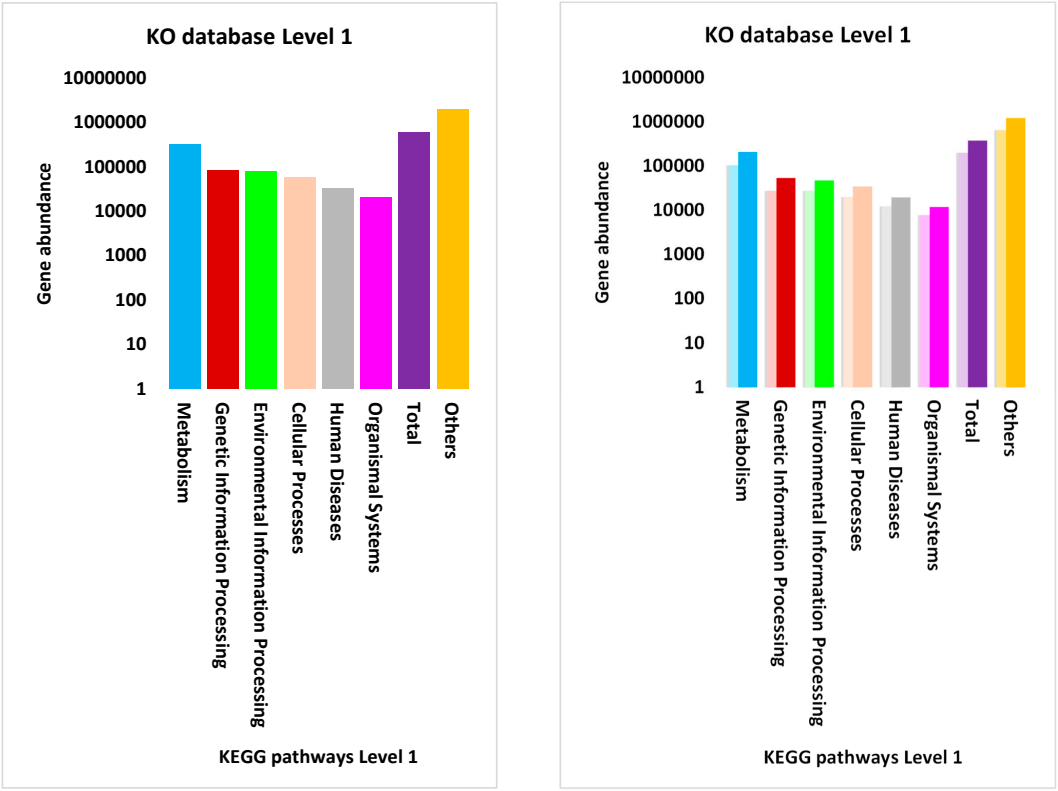

Figure 2. Abundance of genes encoding enzymes of the different functional categories of KO database Level 1 across (**a**) and between (**b**) samples of rhizosphere (R) and surrounding bulk soil (S) microbiomes of *M. oleifera.* Columns with dark colors in (**b**) refer to rhizosphere (R) soil microbiome, while those with light colors refer to microbiome of the surrounding bulk (S) soil. The "others" column refers to genes encoding proteins or enzymes not functioning in KEGG pathways. The data in (**a**) and (**b**) are further described in Figures S1 and S2, respectively, while detailed abundance records are shown in Tables S5 and S8, respectively. Same column color in (**a**) and (**b**) represents same KEGG category.

Table 1. Description of some enriched pathways across rhizosphere and bulk soil microbiomes of *M. oleifera* at the KEGG database Levels 1, 2, and 3 along with pathway IDs.

KEGG Level 1 (Category)	KEGG Level 2 (Sub-Category)	KEGG Level 3 (Pathway) *	Pathway ID
Metabolism	Amino acid metabolism	Arginine biosynthesis	map00220
		Alanine, aspartate, and glutamate metabolism	map00250
		Glycine, serine, and threonine metabolism	map00260
		Cysteine and methionine metabolism	map00270
		Valine, leucine, and isoleucine biosynthesis	map00290
		Lysine biosynthesis	map00300
		Arginine and proline metabolism	map00330
		Histidine metabolism	map00340
		Tyrosine metabolism	map00350
		Phenylalanine metabolism	map00360
		Tryptophan metabolism	map00380
		Phenylalanine, tyrosine, and tryptophan biosynthesis	map00400

Table 1. *Cont.*

KEGG Level 1 (Category)	KEGG Level 2 (Sub-Category)	KEGG Level 3 (Pathway) *	Pathway ID
	Biosynthesis of other secondary metabolites	Staurosporine biosynthesis	Map00404
		Indole alkaloid biosynthesis	map00901
		Biosynthesis of various plant secondary metabolites	Map00999 **
	Carbohydrate metabolism	Starch and sucrose metabolism	map00500
		Inositol phosphate metabolism	map00562
	Energy metabolism	Nitrogen metabolism	map00910
Genetic Information Processing	Translation	Aminoacyl-tRNA biosynthesis	map00970
Cellular Processes	Cellular community—prokaryotes	Quorum sensing	Map02024
	Cell motility	Bacterial chemotaxis	Map02030
Environmental Information Processing	Membrane transport	ABC transporters	map02010

* KEGG pathways involving enriched enzymes at EC level encoded by genes with varying abundance levels are shown in Figures S6–S27. ** A KEGG Pathway that showed very minute abundance, thus is not shown in terms of abundance in Figure 4 and Tables S7 and S10.

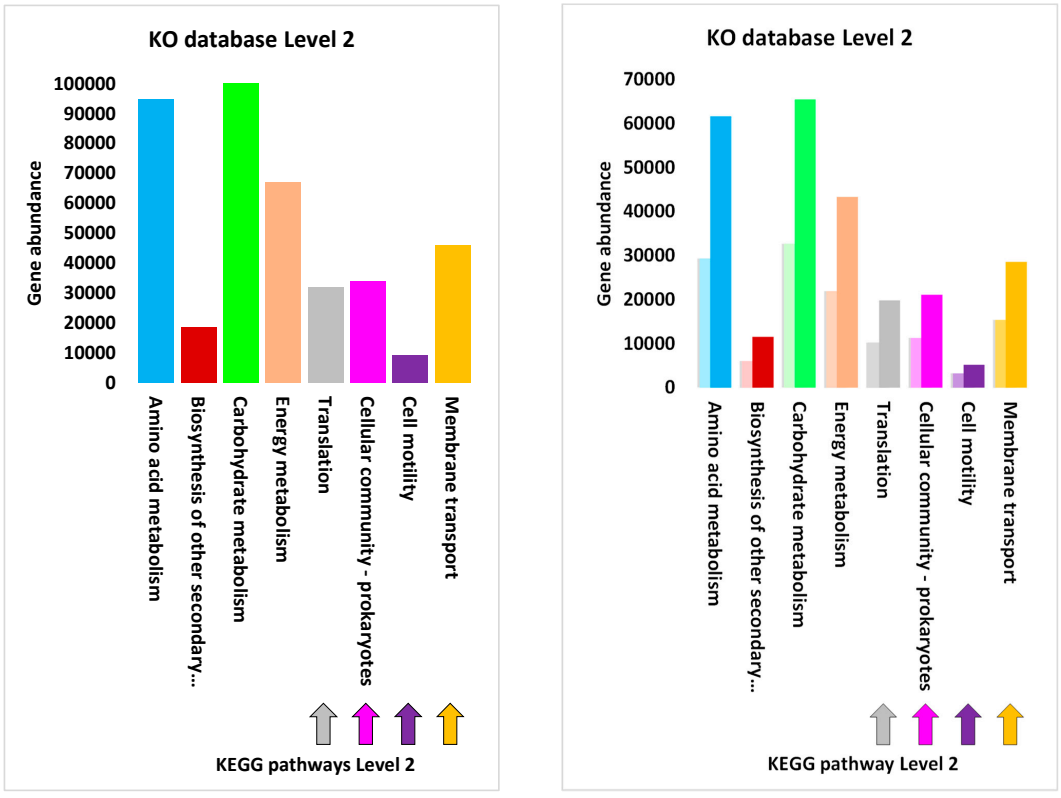

Figure 3. Abundance of genes encoding enzymes of the different functional sub-categories of KEGG database Level 2 across (**a**) and between (**b**) samples of rhizosphere (R) and surrounding bulk soil (S) microbiomes of *M. oleifera*. Columns with dark colors in (**b**) refer to rhizosphere (R) soil microbiome, while those with light colors refer to microbiome of the surrounding bulk (S) soil. All KEGG sub-categories belong to the category "Metabolism", except for the last four sub-categories that belong to categories "Genetic Information Processing" (indicated by the gray arrow), "Cellular Processes" (indicated by the dark pink and violet arrows), and "Environmental Information Processing" (indicated by the orange arrow). The data in (**b**) is further described in Figure S3, while detailed abundance records in (**a**) and (**b**) are shown in Tables S6 and S9, respectively. Same column color in (a) and (b) represents same KEGG category.

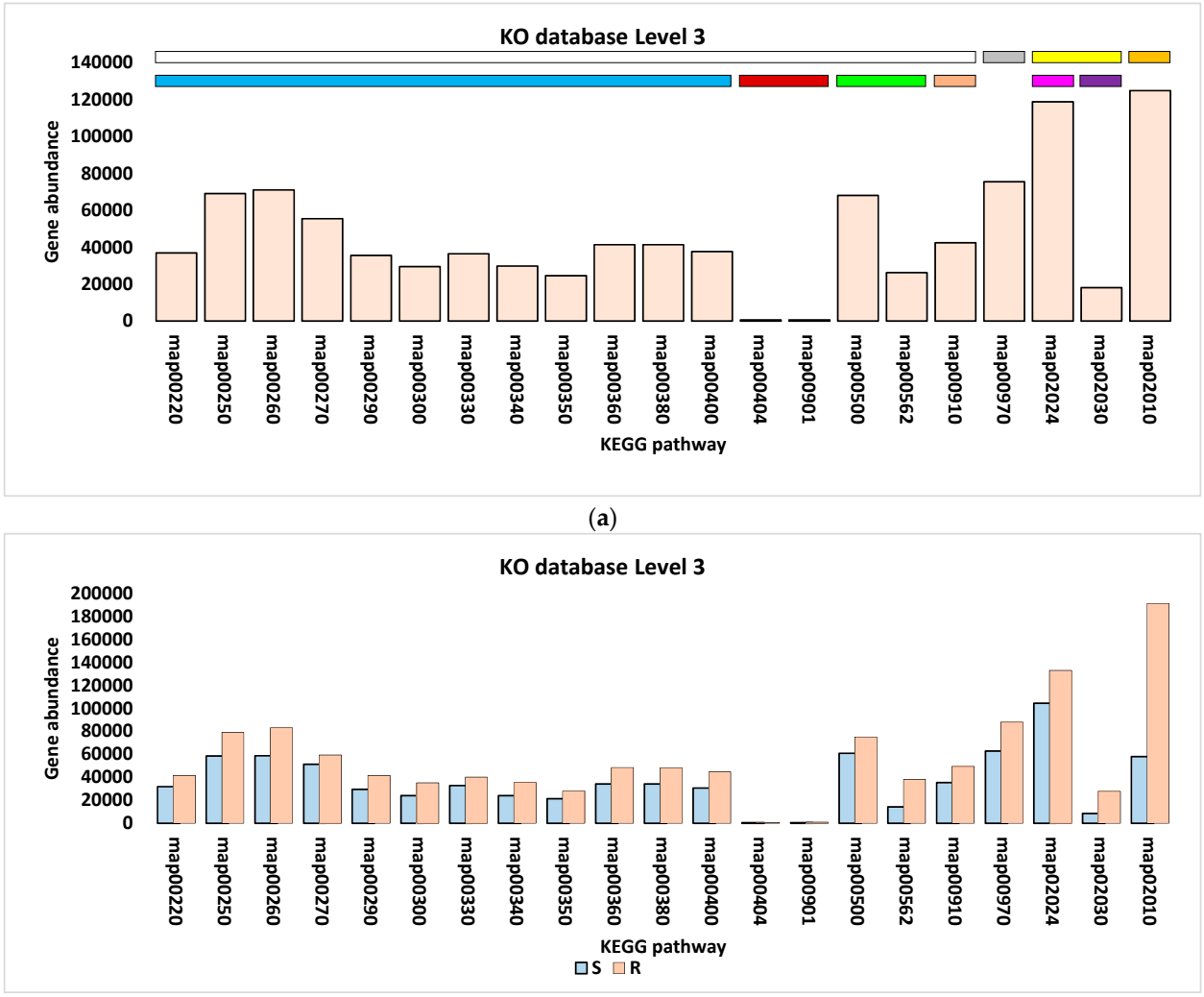

Figure 4. Abundance of genes encoding enzymes of the different functional pathways of KEGG database Level 3 across (**a**) and between (**b**) samples of rhizosphere (R) and surrounding bulk soil (S) microbiomes of *M. oleifera*. KEGG map IDs refer to KEGG pathway identifiers. The white box in (**a**) indicates pathways of the category "Metabolism", while gray, yellow and orange boxes indicate pathways of categories "Genetic Information Processing" (sub-category "Translation"), "Cellular Processes", and "Environmental Information Processing" (sub-category "Membrane transport"), respectively. The sub-categories of "Metabolism" include "Amino acid metabolism" (light blue box), "Biosynthesis of other secondary metabolites" (dark red box), "Carbohydrate metabolism" (light green box), and "Nucleotide metabolism" (light brown box). The sub-categories of "Cellular Processes" include "Quorum sensing" (dark pink box) and "Bacterial chemotaxis" (violet box). The data in (**b**) is further described in Figure S4, while detailed abundance records of (**a**) and (**b**) are shown in Tables S7 and S10, respectively.

The results for the microorganisms along with their enriched enzymes are shown in Table S3, while descriptions of the different enzymes are shown in Table S4. Detailed information regarding gene abundance across and between microbiome samples of either soil type at the category level is shown in Tables S5 and S8, respectively; in Tables S6 and S9 at the sub-category level, respectively; and in Tables S7 and S10 at the KEGG pathway level, respectively.

4. Discussion

The present study focuses on the rhizosphere metagenome of the wild plant *M. oleifera*, as that of domesticated crop plants cannot show the original natural rhizobiome signature, the succession of microbial community assembly, or evolution in the ecosystem [30,31]. This is because the soil of crop plants is subjected to artificial human practices that reshape their rhizobiomes with regard to the type of microbes present and their abundance [23–26]. We focused on microbes in the rhizosphere region in order to study plant-microbe interaction. In this regard, we have studied microbial gene abundance in the rhizosphere and bulk soil, where the chemical composition of these two soil types differs due to plant exudation, which has a temporal/spatial influence on surrounding microbes [30].

4.1. Major Contributors to Plant Growth Parameters and Defense against Phytopathogens in the Rhizosphere Microbiome of M. oleifera

Mutual benefits can be gained for a plant and its rhizosphere microbiome as the latter subsists on the exudates (or rhizodeposits) released from plant roots, while, in return, the plant enables and/or enhances the uptake and recycling of bacterial-processed nutrients by plant roots, and mitigates abiotic stresses [49–51]. In addition, the rhizosphere microbiome participates in the induction of systemic disease resistance, biocontrol, and antibiosis in an antagonistic manner against plant pathogens, while selectively stimulating chemotaxis to promote the endophytic colonization of commensal microbes [52]. However, rhizobacteria are split into functional groups based on their type of interaction with a host plant, which can range from beneficial to pathogenic. Phytopathogens mainly acquire the nutrients required by the host plant [22]. Other pathogens are able to secrete enzymes to biodegrade pectin and cellulose in the plant's cell wall and cause plant soft-rot disease [53,54]. In return, the plant exudes several kinds of compounds to elicit defense actions in the rhizosphere microbiome. Plant exudation methods involve diffusion through the plant cell membrane, active or passive transport for low-molecular-weight compounds (e.g., amino acids, simple sugars, organic acids, etc.), and vesicular transport for high-molecular-weight compounds (e.g., polysaccharides, proteins, etc.) [55]. Under certain conditions, plants efflux amino acids to the soil and block their influx to the root as a defense mechanism against pathogens [56]. A large proportion of exuded or externally introduced amino acids were reported to be incorporated into biomass by soil-dwelling microbes as a weapon against pathogens, while the rest are lost through respiration [57].

Furthermore, plants produce other specific secondary metabolites, which act as antimicrobial compounds to inhibit microbial quorum sensing (QS) and prevent cohabiting phytopathogens from reaching the quorum required to destruct plant cells [58]. QS is a cell-cell communication process that mediates bacterial population density in an environmental niche through the synchronized action of a large number of genes. The expression of these genes is influenced by extracellular signaling molecules named autoinducers (AIs) [59]. These signaling molecules are encoded by a variety of bacterial genes. Gram-negative bacteria usually use acylated homoserine lactone as IAs, while Gram-positive bacteria use oligopeptide permease proteins (Opp) or phosphate-regulator (Phr) peptides, which are cognates of response regulator aspartyl-phosphate (Rap) phosphatases [60–62]. The first IA monitors bacterial population density in quorum sensing [63], while the second participates in the sporulation signal transduction system, particularly in *Bacillus subtilis* [64]. In the present study, the enzyme that synthesizes acylated homoserine lactone, namely acylated homoserine lactone synthase (EC 2.3.1.184), participates in the pathway "Cysteine and methionine metabolism" and is proven to be highly enriched in the *Pseudomonas fluorescens* (Figure S9 and Tables S3 and S11) of the rhizosphere microbiome of *M. oleifera*. In terms of oligopeptide, the results indicated the enrichment of two members (e.g., ComX and ComQ) of the ComQXPA system (Figure S25). This QS system participates in determining the social communication group of *Bacillus subtilis* [65]. This bacterium also uses a QS system, namely Rap-Phr, which participates in attenuating growth based on bacterial density [66]. In the

present study, *Bacillus* seems to have encoded all receptor-signal pairs of this system (e.g., PhrA, PhrC, PhrE, PhrF, PhrG, and PhrK) that promote the production of Opp (Figure S25).

Other functional steps of QS seem to also be enriched in many other microbes in the rhizosphere microbiome of *M. oleifera* including the Gram-negative bacteria *Pseudomonas aeruginosa* and *Escherichia coli,* and the Gram-positive bacteria *Streptococcus* sp. (Figure S25 and Table S3). For example, a type of IAs, namely AI-2, is produced by an enzyme involved in the activated methyl cycle (AMC), namely LuxS protein, in *E. coli* and processed by the *lipolysis-stimulated lipoprotein* (*lsr*) operon [67]. In the present study, this enzyme is enriched in *E. coli* in the rhizosphere microbiome of *M. oleifera* (Figure S25 and Table S3). Several reports indicated that bacterial AIs elicit responses from the host plant by releasing exudates that promote the growth and colonization of the cohabiting commensal microbes [68]. We speculate that an abundance of microbial genes governing QS in the rhizosphere microbiome of *M. oleifera* indicates that the targeting of quorum sensing by the host plant is not meant to be the first-line defensive strategy of plants against phytopathogens, as the abundance of genes encoding QS in the rhizosphere microbiome of *M. oleifera* was higher than that of the bulk soil microbiome (Figures 4 and S4 and Table S10). This might be due to the rare presence of phytopathogens in the rhizosphere of *M. oleifera,* or the plant might utilize other alternative defense mechanisms as the first-line defensive strategy against phytopathogens. The latter statement requires further analysis to support this claim.

On the other hand, beneficial bacteria can undergo symbiotic relationships with host plants and approach a mutual exchange of substrates and metabolites. Examples include atmospheric nitrogen-fixating microbes that convert nitrogen to ammonia and subsequently exchange it for plant-derived carbohydrates [69–71]. Nitrogen that is strongly produced from nitric oxide in the rhizosphere microbiome of *M. oleifera* seems to be efficiently converted into ammonia via the action of a nitrogenase enzyme (EC 1.18.6.1) existing in the pathway "Nitrogen metabolism" (Figure S23). This enzyme is highly enriched (Table S11) in *Pseudomonas fluorescens* (Table S3). The latter kind of bacteria is a plant growth-promoting bacteria (PGPB). As most PGPB inhabit the plant rhizosphere, they are further named PGP-rhizobacteria (PGPR). These bacteria do not have complete dependency on the host plant, but still provide beneficial functions for the plant. For example, they can act in the alteration of plant defense responses and in the production of 1-aminocyclopropane-1-carboxylate (ACC) deaminase (EC 3.5.99.7), which promotes plant root growth and cell elongation and, also, confers tolerance against abiotic stresses [72] by avoiding the accumulation of ethylene [73]. ACC deaminase participates in the pathway "Cysteine and methionine metabolism", where it was shown to be highly enriched in the PGPR *Bacillus subtilis* (Tables S3 and S11), which exists in the rhizosphere microbiome of *M. oleifera* (Figure S9), aligning with results of previous reports [74].

4.2. Chemotaxis in the Rhizosphere Microbiome of M. oleifera

In the present study, *Escherichia coli* was the only microbe that efficiently promoted chemotaxis (Tables S3 and S4), although this process was strongly promoted in the *Bacillus* and *Pseudomonas* species [75]. Chemotaxis is a signal transduction process participating in biofilm formation and colonization of beneficial neutral and mutualistic soil microbes [76]. The presence of these commensal microbes protects plants from pathogens by preventing their colonization [77,78]. The exudation pattern at the plant root-soil interface represents a unique ecological niche that attracts or recruits a large collection of specific microbes that mostly migrate to the rhizosphere via chemotaxis [52,79]. These rhizosphere microbes include Gram-negative (e.g., *Pseudomonas fluorescens* and *Escherichia coli*) and Gram-positive (e.g., *Bacillus subtilis*) bacteria that exhibit motility towards each of the exuded 20 amino acids in addition to certain organic acids, but not towards sugar [80,81]. For example, *Fusarium* wilt infection in watermelon was not severe due to the presence of soil non-pathogenic *Fusarium oxysporum* and *Pseudomonas fluorescens* [82]. In terms of carbohydrate participation in chemotaxis, sucrose was proven to promote solid surface motility (SSM) and root colonization by *B. subtilis* by triggering a signaling cascade in a second pathway

for sucrose utilization, namely "Levan detour" [75]. Thus, it is unlikely that the pathway "Levan detour" exists in the rhizosphere microbiome of *M. oleifera*.

Generally speaking, bacteria sense chemical changes in the surrounding environment using a certain receptor complex that integrates chemical signals in order to modulate the required flagellar direction and swimming mode of bacteria [83,84]. Receptor and flagellar-motor complexes are embedded within the bacterial cell membrane. These actions are mediated by a cascade of transient phosphorylation of chemotaxis proteins transduced via protein-protein interaction and mediated by a shuttle protein, namely CheY [84,85].

There are two kinds of chemotaxis-specific receptors involved in chemotaxis and signal transport, namely methyl-accepting chemotaxis proteins (MCPs) and dual-function receptors. The first type seems to participate in chemotaxis in the rhizosphere microbiome of *M. oleifera* as four MCPs (i.e., Tsr, Tar, Tap, and Aer) which were present in *E. coli* (Figure S26 and Table S3). In accordance with these results, the Tap receptor, in particular, was previously proven to be highly enriched specifically in rhizosphere *E. coli* [86]. The CHeY receptor is a homodimer that is required to connect to a histidine kinase, namely CheA, via a linker protein, namely CheW, in order to generate a stable activated ternary complex [83]. This complex is highly enriched in the rhizosphere microbiome of *M. oleifera* in addition to the MotA stator (Figure S26). The latter is a member of the flagellar-motor complex in addition to MotB, where both combine to form a proton channel anchored to the cell wall in order to promote the flagellar rotation process, which takes place in the *M. oleifera* rhizosphere microbiome. We speculate that rhizobacteria cross talk in order to share metabolites synthesized by specific bacteria (e.g., *E. coli*) to mediate their mobility towards plant exudates.

4.3. Mineral Solubilization in the Rhizosphere Microbiome of M. oleifera

During the symbiotic interaction between plant and rhizosphere microbiome, the latter undergoes several important useful mechanisms, including solubilization to make nutrients in a form available for plant absorption [87]. These mechanisms include several minerals and compounds like phosphorus, nitrogen, potassium, and ammonium and are produced by the rhizosphere microbiomes of the three kingdoms, including archaea, bacteria, and eukarya [51]. Several reports indicated that the solubilization of phosphorus into the form absorbable by roots of green pepper plant takes place in *Pseudomonas fluorescens* by inositol phosphatases and/or several other non-specific phosphate phosphatases and C-P lyases [73]. In addition, *Bacillus subtilis* and *Escherichia coli* can conduct the solubilization of minerals through the production of enzymes that act on organic phosphorus, mainly stored as insoluble myo-inositol hexaphosphate [88–90]. The latter three bacteria were proven to participate in phosphorus solubilization in the rhizosphere of *M. oleifera* as the key player in this mechanism; i.e., myo-inositol-1(or 4)-monophosphatase (EC 3.1.3.25) of the pathway "Inositol phosphate metabolism" was proven to be highly enriched (Figure S22 and Tables S3 and S11).

4.4. Mobility and Restoration of Nutrients in the Rhizosphere Microbiome of M. oleifera

As rhizosphere nutrients are rapidly depleted, a restoration (uptake) action should be conducted by the rhizosphere microbiome to compensate for the shortage. Restoration mainly depends on the relative mobility of nutrients during soil solution movement. For example, nutrients with low rates of mobility (e.g., phosphorus, potassium and ammonium) barely undergo restoration, whereas those with high rates (e.g., nitrate and calcium) are easily restored [91]. Amino acids are the main mobilizable source of carbon and nitrogen that support microbial growth in the rhizosphere compared with other chemicals like sugars or organic acids [52]. As exudates, changes in the level and distribution of amino acids in the soil can effectively alter the signature and function of the microbial community. We speculate that bacteria, under certain conditions, synthesizes and metabolizes amino acids at a high rate in order to provide the plant with different forms of nitrogen, e.g., amino acids, ammonia, nitrite, nitric oxide, and nitrogen (Figures S6–S17 and S23). Then, the rate of

restoration of all forms of nitrogen in the rhizosphere microbiome of *M. oleifera* is expected to be high. Some selected highly enriched enzymes in the rhizosphere microbiome of *M. oleifera* (Table S11) acted in the biosynthesis of all amino acids, while in metabolism of only 14 amino acids, and are shown in Figure 5. Figures S6–S17 indicate cross talking among pathways which handle the dynamics of the biosynthesis/metabolism of amino acids, in which many amino acids are synthesized as a result of the metabolism of other amino acids. For example, alanine can be synthesized by metabolizing aspartate via the action of aspartate 4-decarboxylase (EC 4.1.1.12), as shown in the pathway "Alanine, aspartate and glutamate metabolism" (Figure S7). Additionally, serine aldolase or aminomethyl transferase (EC 2.1.2.1) acts bi-directionally, as shown in the pathway "Glycine, serine and threonine metabolism", towards the biosynthesis/metabolism of serine and glycine, while threonine aldolase (EC 4.1.2.48) also acts bi-directionally towards the biosynthesis/metabolism of glycine (Figure S8). Furthermore, tryptophan can be synthesized by metabolizing serine due to the action of tryptophan synthase (EC 4.2.1.20) as shown in the latter pathway (Figure S8). We speculate that the direction of each reaction should depend on the demands of the rhizosphere microbiome and/or host plant. The first, second, and forth enzymes are highly enriched in the *Bacillus subtilis*, *Pseudomonas fluorescens,* and *E. coli* of the rhizosphere microbiome of *M. oleifera*, while the third enzyme is highly enriched in *E. coli* only (Tables S3 and S11).

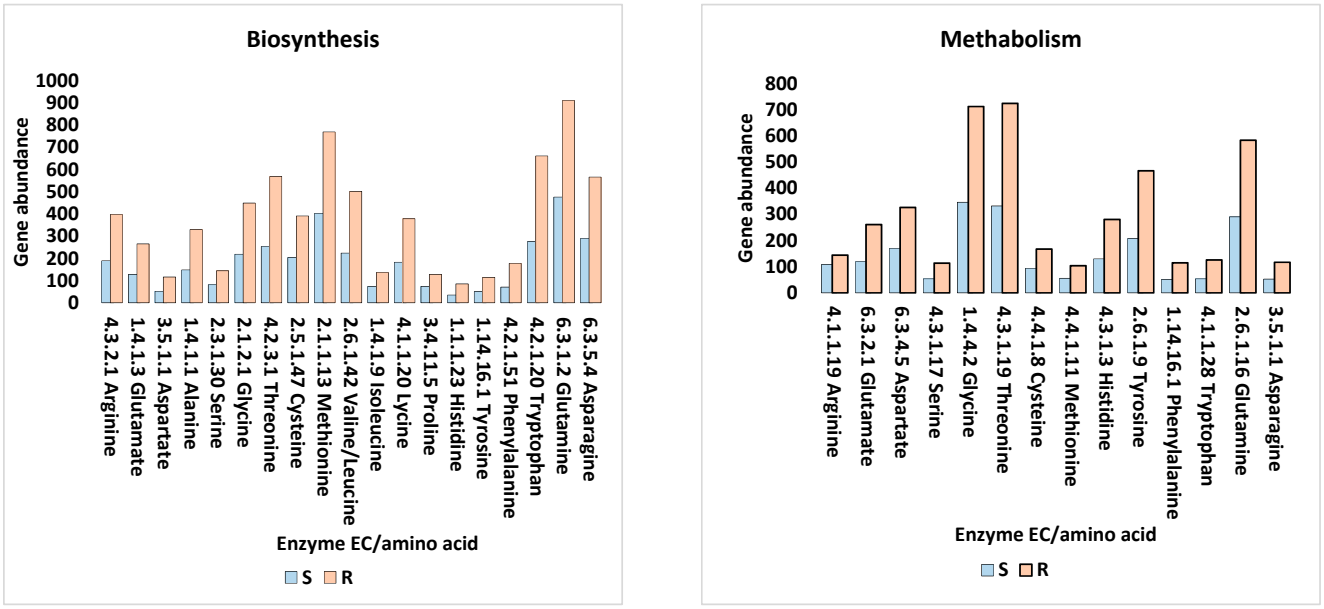

(**a**) (**b**)

Figure 5. Abundance of genes encoding selected highly enriched enzymes in KEGG pathways towards either the biosynthesis (**a**) or metabolism (**b**) of amino acids in the rhizobiome of *M. oleifera*. Detailed information regarding the abundance of genes encoding these and other enzymes in different KEGG pathways is shown in Table S11. Detailed descriptions of these enzyme ECs are given in Table S4. There are several other enzymes that participate in either process and follow the same pattern of gene abundance and enzyme enrichment.

Amino acids were also proven to stand mainly as intermediate switchers or biomarkers for the direction of the soil nitrogen cycle, where their appearance indicates organic matter degradation and release from cells, and their disappearance indicates the mineralization and assimilation, or low mobility and restoration rates [91]. In terms of the relative abundance of free amino acids in rhizosphere soil, a meta-analysis from 22 studies indicated that Ala and Glu are the most abundant free non-protein amino acids across the steps of the nitrogen cycle, followed by Asp, Gln, Gly, His, Leu, Ser, Thr, Val, Arg, and Asn, while the abundance of Met and Cys were the lowest [92]. We speculate that a certain scenario of

cross talking ought to take place between plant root cells and the surrounding rhizosphere microbes in order to rescue nutrients with poor mobility by storing them in the rhizosphere microbiome until they are eventually required by the plant, or the plant, at some point, promotes nutrient mobility in the rhizosphere microbiome by promoting higher rates of biosynthesis, metabolism, and the transportation of the required nutrients.

4.5. Amino Acid Transport in the Rhizosphere Microbiome of M. oleifera

The transportation of amino acids in bacteria is mediated by primary active transport using ABC transporters, but not via diffusion across the plasma membrane [93]. The pathway "ABC transporters" was shown to be enriched in the rhizosphere microbiome of *M. oleifera* (Figure S27 and Table S10). Amino acids, as a mandatory source of nitrogen required by plant, transport themselves across the plant cell membrane by one or more of three complex integral membrane protein classes, namely the LHT family (lysine-histidine-like transporters), AAP family (amino acid permeases), and ProT family (proline transporters), each of which have varying roles in plant amino acid transportation [94]. Among these families, AAP seems to have been chosen by the rhizosphere microbiome of *M. oleifera*, where a complex of four important metabolites (e.g., AapJ, AapQ, AapM, and AapP) was highly enriched in the rhizosphere microbiome of *M. oleifera* (Figure S27). AapJ is known to produce AapQ, an ABC transporter substrate-binding protein, while AapM is known to produce an ABC transporter permease, and AapP is a histidine permease (Figure S27). The latter metabolite is the only among the four transporters with a known EC (EC 7.4.2.1) and is proven in the present study to be highly enriched in *Bacillus subtilis* dwelling in rhizosphere (Tables S3 and S11). This integral ABC transporter complex has a major role in the efflux and transportation of biosynthesized amino acids and other forms of nitrogen source [95].

4.6. Amino Acids and Biofilm Formation in the Rhizosphere Microbiome of M. oleifera

Amino acids produced by bacteria have roles in both bacterial biofilm formation and disassembly in Gram-positive and Gram-negative rhizobacteria [96]. For example, tyrosine synthesized by the highly enriched enzyme in the present study, namely aspartate aminotransferase (EC 2.6.1.1), in the pathway "Tyrosine metabolism" (Figure S14 and Table S11) can decrease cell-cell attachment, and thus primarily prevent biofilm formation. When presented at a low concentration, tyrosine can disassemble biofilm in a number of bacteria, including *Bacillus subtilis* and *Pseudomonas aeruginosa* [97]. The efflux of valine, synthesized in the present study at a high level (Figure S10 and Table S11) by the action of branched-chain amino acid aminotransferase (EC 2.6.1.42) at the pathway "Valine, leucine and isoleucine biosynthesis", also participates in the biofilm formation of certain Gram-negative bacteria [98], although it was proven to be toxic to some bacteria at this high efflux level. Casamino acid, a mixture of all amino acids except for tryptophan and small peptides of hydrolyzed casein, was also proven in an earlier report to promote biofilm formation in the rhizosphere by *Pseudomonas fluorescens* [99].

4.7. Production of Indole Acetic Acid in the Rhizosphere Microbiome of M. oleifera

Indole acetic acid (IAA) is mainly a plant auxin that controls many physiological processes such as cell enlargement, proliferation, and differentiation, as well as the cell's response to light or gravity [100–102]. This auxin was also proven to be synthesized by rhizobacteria, where its level is affected by two factors [103,104]. The first is the location of auxin-synthesizing genes in the bacterial genome, e.g., plasmid or chromosomal, as the first induces higher levels of IAA compared with the second. The second factor is the type of expression, e.g., constitutive or induced, as the first results in higher rate of IAA biosynthesis. IAA can also be synthesized by phytopathogenic bacteria via the best characterized two-step route of the pathway "Tryptophan metabolism", namely indole-3-acetamide (IAM) [88,89], or synthesized by beneficial bacteria via route indole-3-pyruvate (IPyA) of the same pathway [89]. In the present study, plant exudates seem to

promote route IPyA for metabolizing tryptophan, where the two enzymes of this pathway, namely L-tryptophan—pyruvate aminotransferase (EC 2.6.1.99) and indole-3-pyruvate monooxygenase (EC 1.14.31.168), are highly enriched in the *Bacillus subtilis* of the rhizosphere microbiome of *M. oleifera*, whereas the enzymes in the route IAM, i.e., tryptophan 2-monooxygenase (EC 1.13.12.3) and amidase (EC 3.5.1.4), showed almost no enrichment (Figures 6 and S16 and Tables S3 and S11). We speculate that the IPyA route is the choice of the host plant in a trial to bypass deleterious effects of phytopathogens. Similar results were previously reached in blackcurrant with the beneficial rhizobacterium *Pseudomonas fluorescens* [105,106]. To support these results, other prior research indicated that amino acids (e.g., tryptophan, methionine, lysine, and phenylalanine) exuded from alfalfa seedlings and transported to *Salmonella enterica* cells were mainly depleted as a result of de novo amino acid metabolism [107]. The entry of IAA of beneficial bacteria was proven to result in increased rooting, as well as increased ability to uptake minerals in wheat [108]. Another report emphasized the ability of *Pseudomonas putida* to stimulate root elongation in canola via IAA biosynthesis [104]. Prinsen and colleagues [109] also indicated that bacterial IAA mediates rhizobia-plant symbiosis, whereas another report indicated that IAA promotes bacteria's ability to colonize plant roots [104], a role that is mediated by chemotaxis [76].

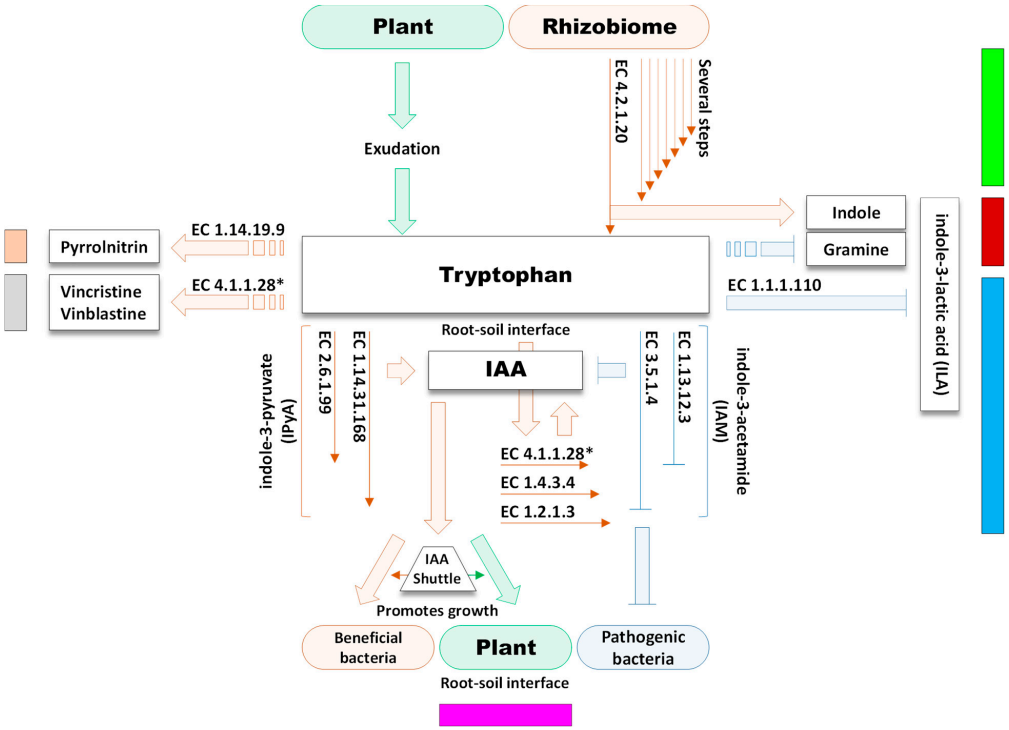

Figure 6. Enrollment of tryptophan in plant-microbe interaction at root-soil interface and its participation in a number of cross-talking pathways in the rhizobiome of *M. oleifera*. Light blue box = pathway "Tryptophan metabolism"; dark red box = pathway "Biosynthesis of various plant secondary metabolites"; light green box = pathway "Phenylalanine, tyrosine and tryptophan biosynthesis"; light brown box = pathway "Staurosporine biosynthesis"; gray box = pathway "Indole alkaloid biosynthesis"; and pink box = pathway "Plant hormone signal transduction". (Clockwise) EC 4.2.1.20 = tryptophan synthase; EC 1.1.1.110 = aromatic 2-oxoacid reductase; EC1.13.12.3 = tryptophan 2-monooxygenase; EC 3.5.1.4 = amidase; EC 4.1.1.28 = aromatic-L- amino-acid decarboxylase; EC 1.4.3.4 = monoamine oxidase; EC 1.2.1.3 = aldehyde dehydrogenase (NAD+); EC 1.14.31.168 = indole-3-pyruvate monooxygenase; EC 2.6.1.99 = L- tryptophan—pyruvate aminotransferase; EC 4.1.1.28 = aromatic-L-amino-acid decarboxylase; and EC1.14.19.9 = tryptophan halogenase. * Indicates an enzyme that participates in the two pathways "Tryptophan metabolism" and "Indole alkaloid biosynthesis" in the rhizobiome of *M. oleifera*.

There is proof that exuded tryptophan is toxic to some bacteria, including the rhizosphere nitrogen-fixing bacterium, *Azospirillum brasilense*. Thus, the process of IAA biosynthesis via beneficial bacteria not only promotes plant growth, but also promotes the survival of these beneficial bacteria in the rhizosphere by detoxifying tryptophan and biosynthesizing IAA [110,111] (Figure 6). In the case of an excessive amount of IAA in the rhizosphere, it is possible that the plant partially stores transported IAA in the form of inactive phytohormone namely indole-3-lactic acid (ILA). This compound is originally synthesized in the rhizobacteria via an irreversible metabolic step mediated by aromatic 2-oxoacid reductase (EC 1.1.1.110) at the pathway "Tryptophan metabolism" (Figure S16). Unlike IAA, the accumulation of cellular ILA in plant cells has a negative influence on plant growth as it competes with plant IAA for auxin-binding sites, which results in a reduced rate of plant growth [112]. In the present study, this step in the pathway does not occur in the rhizosphere microbiome of *M. oleifera*, where aromatic 2-oxoacid reductase does not exist (Figures 6 and S16 and Table S11). Thus, plant cells likely store IAA only. Alternatively, IAA can be stored inside plant tissues in the conjugated form of IAA-amino acids, like lysine, alanine, and leucine [101]. This reaction also takes place for synthesized IAA in bacteria prior being absorbed by plant roots. IAA-lycine is the only conjugate that is shown to exist in the rhizosphere microbiome of *M. oleifera*, where the synthesizing enzyme, indoleacetate—lysine synthetase (EC 6.3.2.20), was enriched in *Pseudomonas fluorescens* and members of the bacterial genera *Microvirga*, *Chloroflexi*, *Streptomyces*, *Arthrobacter*, etc. (Tables S3 and S11). According to our knowledge, the latter enzyme is not a member at any KEGG pathway. IAA-amino acid conjugates might also serve as a storage molecule to be used upon the deficiency of tryptophan at either end [113]. Although there is no solid evidence to support the presence of the IAA conjugated form in the rhizosphere, microbiomes in this region were proven in prior research to harbor enzymes that can both promote IAA-amino acid conjugation and hydrolyze IAA-amino acid peptide bond [114].

In accordance with previous reports, we claim that IAA acts as a shuttle signaling molecule between *M. oleifera* and the surrounding rhizosphere microbiome (Figure 6) with roles in plant-microbe interaction including bacterial colonization, on one hand, and phytostimulation and improvement of plant growth, on the other hand [89,115], where the plant can benefit from IAA synthesized by rhizobacteria, and vice versa. This dynamic interaction is influenced by plant exudate pattern, where IAA efflux/influx is monitored based on the demand at either end.

4.8. Tryptophan as a Core Substrate in a Number of Reactions in the Rhizosphere Microbiome of M. oleifera

We speculate that a plant exudes tryptophan to promote several reactions in the rhizosphere microbiome, on one hand, and to store it along with the bacterially synthesized IAA in the rhizosphere microbiome until required, on the other hand (Figure 6). Tryptophan is a substrate that goes towards the production of IAA in the rhizosphere microbiome of *M. oleifera* not only via route IPyA, but also via a three-step route (Figures 6 and S16). The latter route involves three highly enriched enzymes in the rhizosphere microbiome of *M. oleifera* (Table S11), namely aromatic-L-amino-acid decarboxylase (EC 4.1.1.28), monoamine oxidase (EC 1.4.3.4), and aldehyde dehydrogenase (NAD+) (EC 1.2.1.3), in the pathway "Tryptophan metabolism" (Figure S16). These three enzymes are highly enriched in the present study in *Pseudomonas fluorescens* (Table S3).

Tryptophan is also a substrate in two very important mutual routes of the pathway "Biosynthesis of various plant secondary metabolites" (Figure S20). The first route is Benzoxazinoid biosynthesis, which results in the production of indole via the action of the highly enriched bidirectional enzyme, tryptophan synthase (EC 4.2.1.20), in the rhizosphere microbiome of *M. oleifera* (Table S11). This reaction is not shown in Figure S20, but it was copied from the pathway "Phenylalanine, tyrosine and tryptophan biosynthesis" (Figure S17). The enzyme was highly enriched in the *Bacillus subtilis*, *Pseudomonas fluorescens*, and *E. coli* of the rhizosphere microbiome of *M. oleifera* (Table S3), and in *Pseudomonas putida* in prior

research [116]. Indole is a nitrogen heterocyclic aromatic compound that has important pharmaceutical properties such as being anti-inflammatory, anti-microbial, anti-viral, and anti-cancer [117]. Furthermore, indole-producing rhizobacteria can have applications in biodegradation and bioremediation, where they selectively induce bacterial membrane toxicity and inhibit cell division, ATP production, and protein folding [116]. The second route refers to the eventual biosynthesis of the plant alkaloid gramine via several unassigned steps followed by two assigned steps controlled by the bifunctional enzyme, 3-aminomethylindole N-methyltransferase (EC 2.1.1.340), which is not enriched in the rhizosphere microbiome of *M. oleifera*. Our results align with those of prior reports that indicated that gramine is synthesized by eukaryotic organisms, but can be applied externally as a recruitment cue to promote the assembly of some microbes in the rhizosphere of barley [118].

In the present study, tryptophan also participates in two other important pathways, namely "Staurosporine biosynthesis" (Figure S18) and "Indole alkaloid biosynthesis" (Figure S19). In the first pathway, tryptophan is converted into 7-chloro-L-tryptophan via the highly enriched enzyme, tryptophan halogenase (EC 1.14.19.9), in members of the Gram-negative genus *Sphingomonas* in the rhizosphere microbiome of *M. oleifera* (Tables S3 and S11). This enzyme was previously reported to be enriched in *Pseudomonas fluorescens*, where it participates in the biosynthesis of several medicinally important antibiotics, such as anti-fungal pyrrolnitrin [119]. In the second pathway, tryptophan is converted into tryptamine, a rate-limiting step (Figure S19), via action of the highly enriched enzyme in the rhizosphere microbiome of *M. oleifera* (Table S11), namely aromatic-L-amino-acid decarboxylase (EC 4.1.1.28), which also participates in route IPyA of the pathway "Tryptophan metabolism" (Figures 6 and S16). The pathway "Indole alkaloid biosynthesis" has important pharmaceutical application, like the biosynthesis of the two anti-cancer alkaloids, vincristine and vinblastine [120].

4.9. Role of Amino Acyl tRNA in the Rhizosphere Microbiome of M. oleifera

The growth rate of bacteria is dependent on the proportion of functioning ribosomes out of the total amount of ribosomes acting on protein translation. Excessive unused 70S ribosomes are dimerized by the action of the ribosome modulation factor (RMF) to recover 100S particles. This action protects functioning ribosomes from degradation using proteases and nucleases in the bacterial stationary phase, but results in a reduced translation rate in bacteria due to the loss of amino acyl tRNA binding on such a high-molecular-weight ribosomal particle [121,122]. Thus, a high rate of amino acyl tRNA biosynthesis in the rhizosphere microbiome of *M. oleifera* in the present study (Figure S24 and Table S10) might indicate the existence of a high proportion of functioning 70S particles and a high translation rate.

4.10. Glucose as the Ultimate Target of Carbohydrate Metabolism in M. oleifera

Carbohydrates ultimately break down into glucose via processes of carbohydrate metabolism in order to provide a constant supply of energy to living cells [123]. These processes include biosynthesis, metabolism, and the interconversion of carbohydrates, of which we have selected the pathway "Starch and sucrose metabolism", which is highly enriched in the rhizosphere microbiome of *M. oleifera*, for further discussion (Figures S4 and S21). The main target in this pathway in the rhizosphere microbiome of *M. oleifera* is high enrichment of enzymes that convert sucrose and starch into glucose. The enriched enzymes in the route of sucrose metabolism are α-glucosidase (or maltase) (EC 3.2.1.20), fructokinase (EC 2.7.1.4), glucose-6-phosphate isomerase (EC 5.3.1.9), and glucokinase (EC 2.7.1.2). Meanwhile, the enriched enzymes in the route of starch metabolism are isoamylase (EC 3.2.1.68), (1 -> 4)-alpha-D-glucan (EC 5.4.99.15), maltooligosyltrehalose trehalohydrolase (EC 3.2.1.141), and alpha, alpha-trehalose phosphorylase (EC 2.4.1.64). In the route of sucrose metabolism, the first three enzymes are highly enriched in members of the genus *Microvirga*, while the fourth enzyme, glucokinase, is highly enriched in *E. coli* and *B. subtilis* (Table S3). With

regard to the starch metabolism route, all enzymes are highly enriched in the *B. subtilis* of the rhizosphere microbiome of *M. oleifera* (Tables S3 and S11).

Glucose is a simple monosaccharide that represents the most important carbohydrate form and the primary metabolic fuel of all living organisms. It is usually synthesized in plants from carbon dioxide and water via photosynthesis and can be stored in the plant as starch or broken down to liberate ATP units. The breaking down of glucose starts with glycolysis prior entering Kreb's cycle, and oxidative phosphorylation approaching the generation of several units of ATP [123]. In the other direction, unprocessed glucose serves as the precursor for the biosynthesis of more complex carbohydrates like starch and glycogen [124]. Alternatively, plants can efflux starch, sucrose, and glucose, and their simpler forms, via exudation to the soil by passive diffusion [75,125] in order to form a carbon sink to be available for the plant and its rhizosphere microbiome, collectively called a holobiont [78,126]. These carbon forms can act in chemotaxis as chemo-attractants of soil microbes [127]. Exuded sucrose participates in the plant's defense mechanisms during biotic stresses, as it enhances root colonization of beneficial bacteria such as *B. subtilis* [128,129]. Furthermore, microbes in the rhizosphere microbiome can also synthesize starch and glucose from the atmospheric carbon source and deposit both of them in the soil carbon sink to be mutually shared by the plant and rhizosphere microbiome [126]. In case of a shortage of carbon sources in the plant, we speculate that the plant can recruit starch and glucose from the soil carbon sink to the roots by two known actions, namely cell-wall invertases (CWI) and hexose transporters [130].

5. Conclusions

The present study has focused on the metabolic processes that are enriched in the rhizobiome of the wild plant *M. oleifera* due to the interaction between the plant and the surrounding commensal microbes. The study indicated possible cooperative actions against pathogenic bacteria and mutual benefits at both ends in an orchestrated fashion. However, the exact interactions among soil microbes, on one hand, and between microbes and their host plant, on the other hand, require further experimentation. In addition, we claim that studying the signatures and metabolic capabilities of the plant rhizosphere microbiome of wild plants helps in deciphering new approaches for improving plant growth and defense mechanisms against pathogens. These approaches can be helpful in the breeding program of crop plants in the future.

Supplementary Materials: The following supporting information can be downloaded at: https://drive.google.com/drive/folders/1tnFWf1V3p6rDgHKqg0EHOXKcUUKJuoLR (accessed on 14 October 2022).

Author Contributions: Conceptualization, M.A.T., R.S.J., L.B., M.Y.R., A.S., R.A.A., H.W.A., F.M.A., F.A.A., A.A.B., S.A., A.A.A.; methodology, M.A.T., R.S.J., L.B., M.Y.R., A.S., R.A.A.; software, M.A.T., H.W.A., F.M.A., F.A.A., A.A.B., S.A., A.A.A.; validation, M.A.T., R.S.J., L.B., M.Y.R., A.S., R.A.A.; formal analysis, H.W.A., F.M.A., F.A.A., A.A.B., S.A., A.A.A.; investigation, M.A.T., R.S.J., L.B., M.Y.R., A.S., R.A.A., H.W.A., F.M.A., F.A.A., A.A.B., S.A., A.A.A.; resources, M.A.T., R.S.J., L.B., M.Y.R., A.S., R.A.A., H.W.A., F.M.A., F.A.A., A.A.B., S.A., A.A.A.; data curation, M.A.T., R.S.J., L.B., M.Y.R., A.S., R.A.A., H.W.A.; writing—original draft preparation, H.W.A., F.M.A., F.A.A., A.A.B., S.A., A.A.A.; writing—review and editing, A.A.A.; visualization, M.A.T., R.S.J., L.B., M.Y.R., A.S., R.A.A., H.W.A., F.M.A., F.A.A., A.A.B., S.A., A.A.A.; supervision, H.W.A., F.M.A., F.A.A., A.A.B., S.A., A.A.A.; project administration, M.A.T., R.S.J., L.B., M.Y.R., A.S., R.A.A., H.W.A., F.M.A., F.A.A., A.A.B., S.A., A.A.A.; funding acquisition, M.A.T., R.S.J., L.B., M.Y.R., A.S., R.A.A., H.W.A., F.M.A., F.A.A., A.A.B., S.A., A.A.A. All authors have read and agreed to the published version of the manuscript.

Funding: This work was supported by Princess Nourah bint Abdulrahman University Researchers Supporting Project number (PNURSP2022R31), Princess Nourah bint Abdulrahman University, Riyadh, Saudi Arabia.

Data Availability Statement: Supplemental Data can be accessed at: https://drive.google.com/drive/folders/1tnFWf1V3p6rDgHKqg0EHOXKcUUKJuoLR?usp=sharing (accessed on 24 October 2022).

Conflicts of Interest: The authors declare that the research was conducted in the absence of any commercial or financial relationships that could be construed as a potential conflict of interest.

References

1. Olson, M.; Flora of North America Committee. eFlora summary: Moringaceae: Drumstick family. *Flora N. Am. North Mex.* **2010**, *7*, 167–169.
2. Fozia, F.; Meenu, R.; Avinash, T.; Abdul, A.K.; Shaila, F. Medicinal properties of Moringa oleifera: An overview of promising healer. *J. Med. Plants Res.* **2012**, *6*, 4368–4374.
3. Al-Eisawi, D.M.; Al-Ruzayza, S. The flora of holy Mecca district, Saudi Arabia. *Int. J. Biodivers. Conserv.* **2015**, *7*, 173–189.
4. Gopalakrishnan, L.; Doriya, K.; Kumar, D.S. Moringa oleifera: A review on nutritive importance and its medicinal application. *Food Sci. Hum. Wellness* **2016**, *5*, 49–56. [CrossRef]
5. DeSantis, T.Z.; Hugenholtz, P.; Larsen, N.; Rojas, M.; Brodie, E.L.; Keller, K.; Huber, T.; Dalevi, D.; Hu, P.; Andersen, G.L. Greengenes, a chimera-checked 16S rRNA gene database and workbench compatible with ARB. *Appl. Environ. Microbiol.* **2006**, *72*, 5069–5072. [CrossRef] [PubMed]
6. Carlton, J.M.; Angiuoli, S.V.; Suh, B.B.; Kooij, T.W.; Pertea, M.; Silva, J.C.; Ermolaeva, M.D.; Allen, J.E.; Selengut, J.D.; Koo, H.L.; et al. Genome sequence and comparative analysis of the model rodent malaria parasite Plasmodium yoelii yoelii. *Nature* **2002**, *419*, 512–519. [CrossRef]
7. Chen, C.; Zhou, Y.; Fu, H.; Xiong, X.; Fang, S.; Jiang, H.; Wu, J.; Yang, H.; Gao, J.; Huang, L. Expanded catalog of microbial genes and metagenome-assembled genomes from the pig gut microbiome. *Nat. Commun.* **2021**, *12*, 1106. [CrossRef] [PubMed]
8. Claesson, M.J.; Wang, Q.; O'Sullivan, O.; Greene-Diniz, R.; Cole, J.R.; Ross, R.P.; O'Toole, P.W. Comparison of two next-generation sequencing technologies for resolving highly complex microbiota composition using tandem variable 16S rRNA gene regions. *Nucleic Acids Res.* **2010**, *38*, e200. [CrossRef]
9. Kennedy, N.A.; Walker, A.W.; Berry, S.H.; Duncan, S.H.; Farquarson, F.M.; Louis, P.; Thomson, J.M.; Satsangi, J.; Flint, H.J. The impact of different DNA extraction kits and laboratories upon the assessment of human gut microbiota composition by 16S rRNA gene sequencing. *PLoS ONE* **2014**, *9*, e88982. [CrossRef]
10. Quince, C.; Walker, A.W.; Simpson, J.T.; Loman, N.J.; Segata, N. Shotgun metagenomics, from sampling to analysis. *Nat. Biotechnol.* **2017**, *35*, 833–844. [CrossRef]
11. Tringe, S.G.; von Mering, C.; Kobayashi, A.; Salamov, A.A.; Chen, K.; Chang, H.W.; Podar, M.; Short, J.M.; Mathur, E.J.; Detter, J.C.; et al. Comparative metagenomics of microbial communities. *Science* **2005**, *308*, 554–557. [CrossRef] [PubMed]
12. Raes, J.; Foerstner, K.U.; Bork, P. Get the most out of your metagenome: Computational analysis of environmental sequence data. *Curr. Opin. Microbiol.* **2007**, *10*, 490–498. [CrossRef] [PubMed]
13. Wilkins, L.G.; Ettinger, C.L.; Jospin, G.; Eisen, J.A. Metagenome-assembled genomes provide new insight into the microbial diversity of two thermal pools in Kamchatka, Russia. *Sci. Rep.* **2019**, *9*, 1–15. [CrossRef] [PubMed]
14. Stewart, R.D.; Auffret, M.D.; Warr, A.; Wiser, A.H.; Press, M.O.; Langford, K.W.; Liachko, I.; Snelling, T.J.; Dewhurst, R.J.; Walker, A.W.; et al. Assembly of 913 microbial genomes from metagenomic sequencing of the cow rumen. *Nat. Commun.* **2018**, *9*, 870. [CrossRef]
15. Dilthey, A.T.; Jain, C.; Koren, S.; Phillippy, A.M. Strain-level metagenomic assignment and compositional estimation for long reads with MetaMaps. *Nat. Commun.* **2019**, *10*, 3066. [CrossRef]
16. Scholz, M.; Ward, D.V.; Pasolli, E.; Tolio, T.; Zolfo, M.; Asnicar, F.; Truong, D.T.; Tett, A.; Morrow, A.L.; Segata, N. Strain-level microbial epidemiology and population genomics from shotgun metagenomics. *Nat. Methods* **2016**, *13*, 435–438. [CrossRef]
17. Sugiyama, A.; Ueda, Y.; Zushi, T.; Takase, H.; Yazaki, K. Changes in the bacterial community of soybean rhizospheres during growth in the field. *PLoS ONE* **2014**, *9*, e100709. [CrossRef]
18. Sugiyama, A. The soybean rhizosphere: Metabolites, microbes, and beyond—A review. *J. Adv. Res.* **2019**, *19*, 67–73. [CrossRef]
19. Berendsen, R.L.; Pieterse, C.M.; Bakker, P.A. The rhizosphere microbiome and plant health. *Trends Plant Sci.* **2012**, *17*, 478–486. [CrossRef]
20. Saleem, M.; Law, A.D.; Sahib, M.R.; Pervaiz, Z.H.; Zhang, Q. Impact of root system architecture on rhizosphere and root microbiome. *Rhizosphere* **2018**, *6*, 47–51. [CrossRef]
21. Huang, X.-F.; Chaparro, J.M.; Reardon, K.F.; Zhang, R.; Shen, Q.; Vivanco, J.M. Rhizosphere interactions: Root exudates, microbes, and microbial communities. *Botany* **2014**, *92*, 267–275. [CrossRef]
22. Holden, N. You are what you can find to eat: Bacterial metabolism in the rhizosphere. *Curr. Issues Mol. Biol.* **2019**, *30*, 1–16. [CrossRef] [PubMed]
23. Kolton, M.; Green, S.J.; Harel, Y.M.; Sela, N.; Elad, Y.; Cytryn, E. Draft genome sequence of *Flavobacterium* sp. strain F52, isolated from the rhizosphere of bell pepper (*Capsicum annuum* L. cv. Maccabi). *J. Bacteriol.* **2012**, *194*, 5462–5463. [CrossRef] [PubMed]

24. Yin, C.; Hulbert, S.H.; Schroeder, K.L.; Mavrodi, O.; Mavrodi, D.; Dhingra, A.; Schillinger, W.F.; Paulitz, T.C. Role of bacterial communities in the natural suppression of Rhizoctonia solani bare patch disease of wheat (*Triticum aestivum* L.). *Appl. Environ. Microbiol.* **2013**, *79*, 7428–7438. [CrossRef] [PubMed]
25. Hartman, K.; van der Heijden, M.G.; Roussely-Provent, V.; Walser, J.C.; Schlaeppi, K. Deciphering composition and function of the root microbiome of a legume plant. *Microbiome* **2017**, *5*, 2. [CrossRef]
26. Pérez-Jaramillo, J.E.; Carrión, V.J.; Bosse, M.; Ferrão, L.F.; De Hollander, M.; Garcia, A.A.; Ramírez, C.A.; Mendes, R.; Raaijmakers, J.M. Linking rhizosphere microbiome composition of wild and domesticated Phaseolus vulgaris to genotypic and root phenotypic traits. *ISME J.* **2017**, *11*, 2244–2257. [CrossRef]
27. Schlaeppi, K.; Dombrowski, N.; Oter, R.G.; Ver Loren van Themaat, E.; Schulze-Lefert, P. Quantitative divergence of the bacterial root microbiota in Arabidopsis thaliana relatives. *Proc. Natl. Acad. Sci. USA* **2014**, *111*, 585–592. [CrossRef]
28. Zachow, C.; Müller, H.; Tilcher, R.; Berg, G. Differences between the rhizosphere microbiome of Beta vulgaris ssp. maritima—Ancestor of all beet crops—And modern sugar beets. *Front. Microbiol.* **2014**, *5*, 415. [CrossRef]
29. Bulgarelli, D.; Garrido-Oter, R.; Munch, P.C.; Weiman, A.; Droge, J.; Pan, Y.; McHardy, A.C.; Schulze-Lefert, P. Structure and function of the bacterial root microbiota in wild and domesticated barley. *Cell Host Microbe* **2015**, *17*, 392–403. [CrossRef]
30. Pett-Ridge, J.; Shi, S.; Estera-Molina, K.; Nuccio, E.; Yuan, M.; Rijkers, R.; Swenson, T.; Zhalnina, K.; Northen, T.; Zhou, J. Rhizosphere carbon turnover from cradle to grave: The role of microbe–plant interactions. In *Rhizosphere Biology: Interactions between Microbes and Plants*; Springer: Berlin/Heidelberg, Germany, 2021; pp. 51–73.
31. Pett-Ridge, J.; Firestone, M.K. Using stable isotopes to explore root-microbe-mineral interactions in soil. *Rhizosphere* **2017**, *3*, 244–253. [CrossRef]
32. Hurt, R.A.; Qiu, X.; Wu, L.; Roh, Y.; Palumbo, A.V.; Tiedje, J.M.; Zhou, J. Simultaneous recovery of RNA and DNA from soils and sediments. *Appl. Environ. Microbiol.* **2001**, *67*, 4495–4503. [CrossRef] [PubMed]
33. Mende, D.R.; Waller, A.S.; Sunagawa, S.; Järvelin, A.I.; Chan, M.M.; Arumugam, M.; Raes, J.; Bork, P. Assessment of metagenomic assembly using simulated next generation sequencing data. *PLoS ONE* **2012**, *7*, e31386. [CrossRef] [PubMed]
34. Karlsson, F.H.; Fåk, F.; Nookaew, I.; Tremaroli, V.; Fagerberg, B.; Petranovic, D.; Bäckhed, F.; Nielsen, J. Symptomatic atherosclerosis is associated with an altered gut metagenome. *Nat. Commun.* **2012**, *3*, 1–8. [CrossRef] [PubMed]
35. Oh, J.; Byrd, A.L.; Deming, C.; Conlan, S.; Program, N.C.S.; Kong, H.H.; Segre, J.A. Biogeography and individuality shape function in the human skin metagenome. *Nature* **2014**, *514*, 59–64. [CrossRef]
36. Nielsen, H.B.; Almeida, M.; Juncker, A.S.; Rasmussen, S.; Li, J.; Sunagawa, S.; Plichta, D.R.; Gautier, L.; Pedersen, A.G.; Le Chatelier, E. Identification and assembly of genomes and genetic elements in complex metagenomic samples without using reference genomes. *Nat. Biotechnol.* **2014**, *32*, 822–828. [CrossRef]
37. Li, W.; Godzik, A. Cd-hit: A fast program for clustering and comparing large sets of protein or nucleotide sequences. *Bioinformatics* **2006**, *22*, 1658–1659. [CrossRef]
38. Fu, L.; Niu, B.; Zhu, Z.; Wu, S.; Li, W. CD-HIT: Accelerated for clustering the next-generation sequencing data. *Bioinformatics* **2012**, *28*, 3150–3152. [CrossRef]
39. Li, J.; Jia, H.; Cai, X.; Zhong, H.; Feng, Q.; Sunagawa, S.; Arumugam, M.; Kultima, J.R.; Prifti, E.; Nielsen, T.; et al. An integrated catalog of reference genes in the human gut microbiome. *Nat. Biotechnol.* **2014**, *32*, 834–841. [CrossRef]
40. Huson, D.H.; Beier, S.; Flade, I.; Górska, A.; El-Hadidi, M.; Mitra, S.; Ruscheweyh, H.-J.; Tappu, R. MEGAN community edition-interactive exploration and analysis of large-scale microbiome sequencing data. *PLoS Comput. Biol.* **2016**, *12*, e1004957. [CrossRef]
41. Huson, D.H.; Mitra, S.; Ruscheweyh, H.-J.; Weber, N.; Schuster, S.C. Integrative analysis of environmental sequences using MEGAN4. *Genome Res.* **2011**, *21*, 1552–1560. [CrossRef]
42. Kanehisa, M.; Sato, Y.; Morishima, K. BlastKOALA and GhostKOALA: KEGG Tools for Functional Characterization of Genome and Metagenome Sequences. *J. Mol. Biol.* **2016**, *428*, 726–731. [CrossRef] [PubMed]
43. Kanehisa, M.; Sato, Y.; Kawashima, M.; Furumichi, M.; Tanabe, M. KEGG as a reference resource for gene and protein annotation. *Nucleic Acids Res.* **2016**, *44*, D457–D462. [CrossRef] [PubMed]
44. Kanehisa, M.; Goto, S.; Hattori, M.; Aoki-Kinoshita, K.F.; Itoh, M.; Kawashima, S.; Katayama, T.; Araki, M.; Hirakawa, M. From genomics to chemical genomics: New developments in KEGG. *Nucleic Acids Res.* **2006**, *34*, D354–D357. [CrossRef] [PubMed]
45. Kanehisa, M.; Goto, S.; Sato, Y.; Kawashima, M.; Furumichi, M.; Tanabe, M. Data, information, knowledge and principle: Back to metabolism in KEGG. *Nucleic Acids Res.* **2014**, *42*, D199–D205. [CrossRef]
46. Segata, N.; Izard, J.; Waldron, L.; Gevers, D.; Miropolsky, L.; Garrett, W.S.; Huttenhower, C. Metagenomic biomarker discovery and explanation. *Genome Biol.* **2011**, *12*, R60. [CrossRef] [PubMed]
47. Karlsson, F.H.; Tremaroli, V.; Nookaew, I.; Bergstrom, G.; Behre, C.J.; Fagerberg, B.; Nielsen, J.; Backhed, F. Gut metagenome in European women with normal, impaired and diabetic glucose control. *Nature* **2013**, *498*, 99–103. [CrossRef]
48. Bahieldin, A.; Atef, A.; Sabir, J.S.; Gadalla, N.O.; Edris, S.; Alzohairy, A.M.; Radhwan, N.A.; Baeshen, M.N.; Ramadan, A.M.; Eissa, H.F.; et al. RNA-Seq analysis of the wild barley (*H. spontaneum*) leaf transcriptome under salt stress. *Comptes Rendus Biol.* **2015**, *338*, 285–297. [CrossRef]
49. Naik, K.; Mishra, S.; Srichandan, H.; Singh, P.K.; Sarangi, P.K. Plant growth promoting microbes: Potential link to sustainable agriculture and environment. *Biocatal. Agric. Biotechnol.* **2019**, *21*, 101326. [CrossRef]
50. Lugtenberg, B.; Kamilova, F. Plant-growth-promoting rhizobacteria. *Annu. Rev. Microbiol.* **2009**, *63*, 541–556. [CrossRef]

51. Devi, R.; Kaur, T.; Kour, D.; Yadav, A.; Yadav, A.N.; Suman, A.; Ahluwalia, A.S.; Saxena, A.K. Minerals solubilizing and mobilizing microbiomes: A sustainable approaches for managing minerals deficiency in agricultural soil. *J. Appl. Microbiol.* **2022**, *133*, 1245–1272. [CrossRef]
52. Moe, L.A. Amino acids in the rhizosphere: From plants to microbes. *Am. J. Bot.* **2013**, *100*, 1692–1705. [CrossRef]
53. Harris, S.J.; Shih, Y.L.; Bentley, S.D.; Salmond, G.P. The hexA gene of Erwinia carotovora encodes a LysR homologue and regulates motility and the expression of multiple virulence determinants. *Mol. Microbiol.* **1998**, *28*, 705–717. [CrossRef]
54. Silby, M.W.; Cerdeno-Tarraga, A.M.; Vernikos, G.S.; Giddens, S.R.; Jackson, R.W.; Preston, G.M.; Zhang, X.X.; Moon, C.D.; Gehrig, S.M.; Godfrey, S.A.; et al. Genomic and genetic analyses of diversity and plant interactions of Pseudomonas fluorescens. *Genome Biol.* **2009**, *10*, R51. [CrossRef]
55. Badri, D.V.; Quintana, N.; El Kassis, E.G.; Kim, H.K.; Choi, Y.H.; Sugiyama, A.; Verpoorte, R.; Martinoia, E.; Manter, D.K.; Vivanco, J.M. An ABC transporter mutation alters root exudation of phytochemicals that provoke an overhaul of natural soil microbiota. *Plant Physiol.* **2009**, *151*, 2006–2017. [CrossRef]
56. Hartmann, N.; Erbs, M.; Forrer, H.R.; Vogelgsang, S.; Wettstein, F.E.; Schwarzenbach, R.P.; Bucheli, T.D. Occurrence of zearalenone on Fusarium graminearum infected wheat and maize fields in crop organs, soil, and drainage water. *Environ. Sci. Technol.* **2008**, *42*, 5455–5460. [CrossRef]
57. Jones, D.; Kemmitt, S.; Wright, D.; Cuttle, S.; Bol, R.; Edwards, A. Rapid intrinsic rates of amino acid biodegradation in soils are unaffected by agricultural management strategy. *Soil Biol. Biochem.* **2005**, *37*, 1267–1275. [CrossRef]
58. Rudrappa, T.; Bais, H.P. Curcumin, a known phenolic from Curcuma longa, attenuates the virulence of Pseudomonas aeruginosa PAO1 in whole plant and animal pathogenicity models. *J. Agric. Food Chem.* **2008**, *56*, 1955–1962. [CrossRef]
59. Rutherford, S.T.; Bassler, B.L. Bacterial quorum sensing: Its role in virulence and possibilities for its control. *Cold Spring Harb. Perspect. Med.* **2012**, *2*, a012427. [CrossRef]
60. Torres-Cerna, C.E.; Morales, J.A.; Hernandez-Vargas, E.A. Modeling Quorum Sensing Dynamics and Interference on Escherichia coli. *Front Microbiol.* **2019**, *10*, 1835. [CrossRef]
61. Ng, W.L.; Bassler, B.L. Bacterial quorum-sensing network architectures. *Annu. Rev. Genet.* **2009**, *43*, 197–222. [CrossRef]
62. Williams, P.; Camara, M. Quorum sensing and environmental adaptation in Pseudomonas aeruginosa: A tale of regulatory networks and multifunctional signal molecules. *Curr. Opin. Microbiol.* **2009**, *12*, 182–191. [CrossRef]
63. Parsek, M.R.; Val, D.L.; Hanzelka, B.L.; Cronan, J.E., Jr.; Greenberg, E.P. Acyl homoserine-lactone quorum-sensing signal generation. *Proc. Natl. Acad. Sci. USA* **1999**, *96*, 4360–4365. [CrossRef]
64. Perego, M.; Glaser, P.; Hoch, J.A. Aspartyl-phosphate phosphatases deactivate the response regulator components of the sporulation signal transduction system in Bacillus subtilis. *Mol. Microbiol.* **1996**, *19*, 1151–1157. [CrossRef]
65. Kalamara, M.; Spacapan, M.; Mandic-Mulec, I.; Stanley-Wall, N.R. Social behaviours by Bacillus subtilis: Quorum sensing, kin discrimination and beyond. *Mol. Microbiol.* **2018**, *110*, 863–878. [CrossRef]
66. Gallegos-Monterrosa, R.; Christensen, M.N.; Barchewitz, T.; Koppenhofer, S.; Priyadarshini, B.; Balint, B.; Maroti, G.; Kempen, P.J.; Dragos, A.; Kovacs, A.T. Impact of Rap-Phr system abundance on adaptation of Bacillus subtilis. *Commun. Biol.* **2021**, *4*, 468. [CrossRef]
67. De Keersmaecker, S.C.; Sonck, K.; Vanderleyden, J. Let LuxS speak up in AI-2 signaling. *Trends Microbiol.* **2006**, *14*, 114–119. [CrossRef]
68. Miller, M.B.; Bassler, B.L. Quorum sensing in bacteria. *Annu. Rev. Microbiol.* **2001**, *55*, 165–199. [CrossRef]
69. Hayat, R.; Ali, S.; Amara, U.; Khalid, R.; Ahmed, I. Soil beneficial bacteria and their role in plant growth promotion: A review. *Ann. Microbiol.* **2010**, *60*, 579–598. [CrossRef]
70. James, E. Nitrogen fixation in endophytic and associative symbiosis. *Field Crops Res.* **2000**, *65*, 197–209. [CrossRef]
71. de Bruijn, F.J. The quest for biological nitrogen fixation in cereals: A perspective and prospective. *Biol. Nitrogen Fixat.* **2015**, 1087–1101.
72. Duan, B.; Li, L.; Chen, G.; Su-Zhou, C.; Li, Y.; Merkeryan, H.; Liu, W.; Liu, X. 1-Aminocyclopropane-1-Carboxylate Deaminase-Producing Plant Growth-Promoting Rhizobacteria Improve Drought Stress Tolerance in Grapevine (*Vitis vinifera* L.). *Front. Plant Sci.* **2021**, *12*, 706990.
73. Shen, X.; Hu, H.; Peng, H.; Wang, W.; Zhang, X. Comparative genomic analysis of four representative plant growth-promoting rhizobacteria in Pseudomonas. *BMC Genom.* **2013**, *14*, 271. [CrossRef]
74. Blake, C.; Christensen, M.N.; Kovacs, A.T. Molecular Aspects of Plant Growth Promotion and Protection by Bacillus subtilis. *Mol. Plant Microbe Interact.* **2021**, *34*, 15–25. [CrossRef] [PubMed]
75. Tian, T.; Sun, B.; Shi, H.; Gao, T.; He, Y.; Li, Y.; Liu, Y.; Li, X.; Zhang, L.; Li, S.; et al. Sucrose triggers a novel signaling cascade promoting Bacillus subtilis rhizosphere colonization. *ISME J.* **2021**, *15*, 2723–2737. [CrossRef]
76. Mishra, S.; Upadhyay, R.S.; Nautiyal, C.S. Unravelling the beneficial role of microbial contributors in reducing the allelopathic effects of weeds. *Appl. Microbiol. Biotechnol.* **2013**, *97*, 5659–5668. [CrossRef]
77. Andreote, F.D.; Gumiere, T.; Durrer, A. Exploring interactions of plant microbiomes. *Sci. Agrícola* **2014**, *71*, 528–539. [CrossRef]
78. Vandenkoornhuyse, P.; Quaiser, A.; Duhamel, M.; Le Van, A.; Dufresne, A. The importance of the microbiome of the plant holobiont. *New Phytol.* **2015**, *206*, 1196–1206. [CrossRef]
79. Doornbos, R.F.; van Loon, L.C.; Bakker, P.A. Impact of root exudates and plant defense signaling on bacterial communities in the rhizosphere. A review. *Agron. Sustain. Dev.* **2012**, *32*, 227–243. [CrossRef]

80. Oku, S.; Komatsu, A.; Tajima, T.; Nakashimada, Y.; Kato, J. Identification of chemotaxis sensory proteins for amino acids in Pseudomonas fluorescens Pf0-1 and their involvement in chemotaxis to tomato root exudate and root colonization. *Microbes Environ.* **2012**, *27*, ME12005. [CrossRef]
81. de Weert, S.; Vermeiren, H.; Mulders, I.H.; Kuiper, I.; Hendrickx, N.; Bloemberg, G.V.; Vanderleyden, J.; De Mot, R.; Lugtenberg, B.J. Flagella-driven chemotaxis towards exudate components is an important trait for tomato root colonization by Pseudomonas fluorescens. *Mol. Plant-Microbe Interact.* **2002**, *15*, 1173–1180. [CrossRef]
82. Alabouvette, C.; Couteaudier, Y. Biological control of Fusarium wilts with nonpathogenic Fusaria. *Biol. Control. Plant Dis.* **1992**, 415–426.
83. Falke, J.J.; Bass, R.B.; Butler, S.L.; Chervitz, S.A.; Danielson, M.A. The two-component signaling pathway of bacterial chemotaxis: A molecular view of signal transduction by receptors, kinases, and adaptation enzymes. *Annu. Rev. Cell Dev. Biol.* **1997**, *13*, 457–512. [CrossRef] [PubMed]
84. Bren, A.; Eisenbach, M. How signals are heard during bacterial chemotaxis: Protein-protein interactions in sensory signal propagation. *J. Bacteriol.* **2000**, *182*, 6865–6873. [CrossRef] [PubMed]
85. Bourret, R.B.; Hess, J.F.; Borkovich, K.A.; Pakula, A.A.; Simon, M.I. Protein phosphorylation in chemotaxis and two-component regulatory systems of bacteria. *J. Biol. Chem.* **1989**, *264*, 7085–7088. [CrossRef]
86. Bibikov, S.I.; Biran, R.; Rudd, K.E.; Parkinson, J.S. A signal transducer for aerotaxis in Escherichia coli. *J. Bacteriol.* **1997**, *179*, 4075–4079. [CrossRef] [PubMed]
87. Divjot, K.; Rana, K.L.; Tanvir, K.; Yadav, N.; Yadav, A.N.; Kumar, M.; Kumar, V.; Dhaliwal, H.S.; Saxena, A.K. Biodiversity, current developments and potential biotechnological applications of phosphorus-solubilizing and-mobilizing microbes: A review. *Pedosphere* **2021**, *31*, 43–75.
88. Costacurta, A.; Vanderleyden, J. Synthesis of phytohormones by plant-associated bacteria. *Crit. Rev. Microbiol.* **1995**, *21*, 1–18. [CrossRef]
89. Spaepen, S.; Vanderleyden, J.; Remans, R. Indole-3-acetic acid in microbial and microorganism-plant signaling. *FEMS Microbiol. Rev.* **2007**, *31*, 425–448. [CrossRef]
90. Francis, I.; Holsters, M.; Vereecke, D. The Gram-positive side of plant–microbe interactions. *Environ. Microbiol.* **2010**, *12*, 1–12. [CrossRef] [PubMed]
91. Neumann, G.; Römheld, V. Root-induced changes in the availability of nutrients in the rhizosphere. *Plant Roots Hidden Half* **2002**, 617–649.
92. Vranova, V.; Rejsek, K.; Skene, K.R.; Formanek, P. Non-protein amino acids: Plant, soil and ecosystem interactions. *Plant Soil* **2011**, *342*, 31–48. [CrossRef]
93. Saier, M.H., Jr. Families of transmembrane transporters selective for amino acids and their derivatives the information presented in this review was initially prepared for presentation at the FASEB meeting on amino acid transport held in Copper Mountain, Colorado, June 26–July 1, 1999 and was updated in January 2000 following the meeting of the Transport Nomenclature Panel of the International Union of Biochemistry and Molecular Biology (IUBMB) in Geneva, November 28–30, 1999. The system of classification described in this review reflects the recommendations of that panel. *Microbiology* **2000**, *146*, 1775–1795. [PubMed]
94. Tegeder, M. Transporters for amino acids in plant cells: Some functions and many unknowns. *Curr. Opin. Plant Biol.* **2012**, *15*, 315–321. [CrossRef] [PubMed]
95. Tian, M.; Bao, Y.; Li, P.; Hu, H.; Ding, C.; Wang, S.; Li, T.; Qi, J.; Wang, X.; Yu, S. The putative amino acid ABC transporter substrate-binding protein AapJ2 is necessary for Brucella virulence at the early stage of infection in a mouse model. *Vet. Res.* **2018**, *49*, 1–11. [CrossRef]
96. Kolodkin-Gal, I.; Romero, D.; Cao, S.; Clardy, J.; Kolter, R.; Losick, R. D-amino acids trigger biofilm disassembly. *Science* **2010**, *328*, 627–629. [CrossRef]
97. Roy, R.; Tiwari, M.; Donelli, G.; Tiwari, V. Strategies for combating bacterial biofilms: A focus on anti-biofilm agents and their mechanisms of action. *Virulence* **2018**, *9*, 522–554. [CrossRef]
98. Valle, J.; Da Re, S.; Schmid, S.; Skurnik, D.; d'Ari, R.; Ghigo, J.-M. The amino acid valine is secreted in continuous-flow bacterial biofilms. *J. Bacteriol.* **2008**, *190*, 264–274. [CrossRef] [PubMed]
99. O'Toole, G.A.; Kolter, R. Initiation of biofilm formation in Pseudomonas fluorescens WCS365 proceeds via multiple, convergent signalling pathways: A genetic analysis. *Mol. Microbiol.* **1998**, *28*, 449–461. [CrossRef]
100. Staswick, P.E. The tryptophan conjugates of jasmonic and indole-3-acetic acids are endogenous auxin inhibitors. *Plant Physiol.* **2009**, *150*, 1310–1321. [CrossRef]
101. Woodward, A.W.; Bartel, B. Auxin: Regulation, action, and interaction. *Ann. Bot.* **2005**, *95*, 707–735. [CrossRef]
102. Teale, W.D.; Paponov, I.A.; Palme, K. Auxin in action: Signalling, transport and the control of plant growth and development. *Nat. Rev. Mol. Cell Biol.* **2006**, *7*, 847–859. [CrossRef] [PubMed]
103. Brandl, M.T.; Lindow, S.E. Environmental signals modulate the expression of an indole-3-acetic acid biosynthetic gene in Erwinia herbicola. *Mol. Plant-Microbe Interact.* **1997**, *10*, 499–505. [CrossRef]
104. Patten, C.L.; Glick, B.R. Role of Pseudomonas putida indoleacetic acid in development of the host plant root system. *Appl. Environ. Microbiol.* **2002**, *68*, 3795–3801. [CrossRef] [PubMed]

105. Dubeikovsky, A.; Mordukhova, E.; Kochetkov, V.t.; Polikarpova, F.; Boronin, A. Growth promotion of blackcurrant softwood cuttings by recombinant strain Pseudomonas fluorescens BSP53a synthesizing an increased amount of indole-3-acetic acid. *Soil Biol. Biochem.* **1993**, *25*, 1277–1281. [CrossRef]
106. Persello-Cartieaux, F.; Nussaume, L.; Robaglia, C. Tales from the underground: Molecular plant–rhizobacteria interactions. *Plant Cell Environ.* **2003**, *26*, 189–199. [CrossRef]
107. Kwan, G.; Pisithkul, T.; Amador-Noguez, D.; Barak, J. De novo amino acid biosynthesis contributes to salmonella enterica growth in Alfalfa seedling exudates. *Appl. Environ. Microbiol.* **2015**, *81*, 861–873. [CrossRef]
108. Dobbelaere, S.; Croonenborghs, A.; Thys, A.; Vande Broek, A.; Vanderleyden, J. Phytostimulatory effect of Azospirillum brasilense wild type and mutant strains altered in IAA production on wheat. *Plant Soil* **1999**, *212*, 153–162. [CrossRef]
109. Prinsen, E.; Chauvaux, N.; Schmidt, J.; John, M.; Wieneke, U.; De Greef, J.; Schell, J.; Van Onckelen, H. Stimulation of indole-3-acetic acid production in Rhizobium by flavonoids. *FEBS Lett.* **1991**, *282*, 53–55. [CrossRef]
110. BAR, T.; OKON, Y. Induction of indole-3-acetic acid synthesis and possible toxicity of tryptophan in Azospirillum brasilense Sp7. *Symbiosis* **1992**, *13*, 191–198.
111. Steenhoudt, O.; Vanderleyden, J. Azospirillum, a free-living nitrogen-fixing bacterium closely associated with grasses: Genetic, biochemical and ecological aspects. *FEMS Microbiol. Rev.* **2000**, *24*, 487–506. [CrossRef]
112. Sprunck, S.; Jacobsen, H.-J.; Reinard, T. Indole-3-lactic acid is a weak auxin analogue but not an anti-auxin. *J. Plant Growth Regul.* **1995**, *14*, 191–197. [CrossRef]
113. Glass, N.L.; Kosuge, T. Cloning of the gene for indoleacetic acid-lysine synthetase from Pseudomonas syringae subsp. savastanoi. *J. Bacteriol.* **1986**, *166*, 598–603. [CrossRef] [PubMed]
114. Chou, J.-C.; Huang, Y.-B. Induction and characterization of an indole-3-acetyl-L-alanine hydrolase from Arthrobacter ilicis. *J. Plant Growth Regul.* **2005**, *24*, 11–18. [CrossRef]
115. Lambrecht, M.; Okon, Y.; Broek, A.V.; Vanderleyden, J. Indole-3-acetic acid: A reciprocal signalling molecule in bacteria–plant interactions. *Trends Microbiol.* **2000**, *8*, 298–300. [CrossRef]
116. Kim, J.; Hong, H.; Heo, A.; Park, W. Indole toxicity involves the inhibition of adenosine triphosphate production and protein folding in Pseudomonas putida. *FEMS Microbiol. Lett.* **2013**, *343*, 89–99. [CrossRef]
117. Ma, Q.; Zhang, X.; Qu, Y. Biodegradation and Biotransformation of Indole: Advances and Perspectives. *Front Microbiol.* **2018**, *9*, 2625. [CrossRef]
118. Maver, M.; Escudero-Martinez, C.; Abbott, J.; Morris, J.; Hedley, P.E.; Mimmo, T.; Bulgarelli, D. Applications of the indole-alkaloid gramine modulate the assembly of individual members of the barley rhizosphere microbiota. *PeerJ* **2021**, *9*, e12498. [CrossRef]
119. Burd, V.N.; Van Pee, K.H. Halogenating enzymes in the biosynthesis of antibiotics. *Biochemistry* **2003**, *68*, 1132–1135. [CrossRef]
120. Alam, M.M.; Naeem, M.; Khan, M.; Uddin, M. Vincristine and vinblastine anticancer catharanthus alkaloids: Pharmacological applications and strategies for yield improvement. In *Catharanthus Roseus*; Springer: Berlin/Heidelberg, Germany, 2017; pp. 277–307.
121. Wada, A. Growth phase coupled modulation of Escherichia coli ribosomes. *Genes Cells* **1998**, *3*, 203–208. [CrossRef]
122. Crozier, L.; Hedley, P.E.; Morris, J.; Wagstaff, C.; Andrews, S.C.; Toth, I.; Jackson, R.W.; Holden, N.J. Whole-transcriptome analysis of verocytotoxigenic Escherichia coli O157: H7 (Sakai) suggests plant-species-specific metabolic responses on exposure to spinach and lettuce extracts. *Front. Microbiol.* **2016**, *7*, 1088.
123. Maughan, R. Carbohydrate metabolism. *Surgery* **2009**, *27*, 6–10.
124. Nakrani, M.N.; Wineland, R.H.; Anjum, F. *Physiology, Glucose Metabolism*; StatPearls Publishing: Treasure Island, FL, USA, 2020.
125. Chaudhuri, B.; Hörmann, F.; Lalonde, S.; Brady, S.M.; Orlando, D.A.; Benfey, P.; Frommer, W.B. Protonophore-and pH-insensitive glucose and sucrose accumulation detected by FRET nanosensors in Arabidopsis root tips. *Plant J.* **2008**, *56*, 948–962. [CrossRef]
126. Lemoine, R.; La Camera, S.; Atanassova, R.; Dedaldechamp, F.; Allario, T.; Pourtau, N.; Bonnemain, J.L.; Laloi, M.; Coutos-Thevenot, P.; Maurousset, L.; et al. Source-to-sink transport of sugar and regulation by environmental factors. *Front Plant Sci.* **2013**, *4*, 272. [CrossRef] [PubMed]
127. Badri, D.V.; Chaparro, J.M.; Zhang, R.; Shen, Q.; Vivanco, J.M. Application of natural blends of phytochemicals derived from the root exudates of Arabidopsis to the soil reveal that phenolic-related compounds predominantly modulate the soil microbiome. *J. Biol. Chem.* **2013**, *288*, 4502–4512. [CrossRef] [PubMed]
128. Ward, J.M.; Kühn, C.; Tegeder, M.; Frommer, W.B. Sucrose transport in higher plants. *Int. Rev. Cytol.* **1997**, *178*, 41–71.
129. Bais, H.P.; Fall, R.; Vivanco, J.M. Biocontrol of Bacillus subtilis against infection of Arabidopsis roots by Pseudomonas syringae is facilitated by biofilm formation and surfactin production. *Plant Physiol.* **2004**, *134*, 307–319. [CrossRef]
130. Veillet, F.; Gaillard, C.; Coutos-Thevenot, P.; La Camera, S. Targeting the AtCWIN1 Gene to Explore the Role of Invertases in Sucrose Transport in Roots and during Botrytis cinerea Infection. *Front Plant Sci.* **2016**, *7*, 1899. [CrossRef]